PHILOSOPHICAL TRANSACTIONS OF THE ROYAL SOCIETY A MATHEMATICAL, PHYSICAL & ENGINEERING SCIENCES

The Troodos Massif, Cyprus and other Ophiolites as Oceanic Crust: Evaluation and Implications

E. M. Moores and F. J. Vine

Phil. Trans. R. Soc. Lond. A 1971 **268**, 443-467
doi: 10.1098/rsta.1971.0006

Phil. Trans. Roy. Soc. Lond. A. **268**, 443–466 (1971) [443]
Printed in Great Britain

The Troodos Massif, Cyprus and other ophiolites as oceanic crust: evaluation and implications

By E. M. Moores
Department of Geology, University of California, Davis, U.S.A.
and F. J. Vine*
Department of Geological and Geophysical Sciences, Princeton University, U.S.A.

[Plate 5 and 6]

Many Alpine ophiolite complexes characteristically display a pseudostratiform sequence of ultramafics, gabbro, diabase, pillow lava and deep-sea sediments. These masses resemble the known rock suite from the ocean floor. They are either fragments of old oceanic crust and mantle caught up in deformed belts, or results of diapiric emplacement of partly molten mantle material on or near the sea bottom. Such complexes are widespread in the Tethyan mountain system and have been recognized also from the circum-Pacific region. The Troodos Massif, Cyprus, consists of a pseudostratiform mass of harzburgite, dunite, pyroxenite, gabbro, quartz diorite, diabase and pillow lava arranged in a dome-like manner. The diabase forms a remarkable dyke swarm, trending mostly north–south in which 100 km of extension is indicated over 100 km of exposure. Such a feature suggests formation by sea-floor spreading. Layering of pyroxenite, harzburgite and dunite generally is perpendicular to subhorizontal rock unit contacts. The harzburgite and dunite are tectonites and probably represent uppermost mantle. Pyroxenite, gabbro, quartz diorite and diabase may represent the products of partial fusion of mantle material or of fractional crystallization of such partial fusion products. Chemical compositions of mafic intrusive and extrusive rocks do not fit well with oceanic tholeiite compositions, but resemble greenstones and associated rocks recently reported from the oceans.

The massif probably formed about an old Tethyan ridge. Some pillow lavas may be crust added after the main spreading episode. A fault zone active during emplacement of the lower units of the complex may represent a fossil transform fault. Complex chilled margins in the dyke swarms and mutually contradictory cross-cutting relations between dykes and plutonic mafic rock suggest formation of ocean crust by multiple intrusion of small portions of liquid. Uneven top surface of the dyke swarm and some conjugate dyke systems suggest independently varying rates of magma supply and extension.

Other Tethyan ophiolites, particularly in Greece and Italy, exhibit internal structure parallel to, rather than perpendicular to, major rock units, and some show much less diversity in mafic rock type. If these masses are fragments of ocean floor and mantle, such differences in internal structure may be due to differences in spreading processes—perhaps differences in spreading rate.

Introduction

'...in Cyprus there is apparently no sign of a floor of country rocks occurring at the base of the Troodos plutonic rocks. The very high positive gravity anomaly... existing in the Troodos area is an indication that, at least in southern Cyprus, the granitic layer of the earth's crust is missing. The sialic crust...appears to have moved aside under great tensional stress while the numerous dykes of the diabase and pillow lava series were intruded' (Wilson 1959, p. 126).

'The dykes, as the lava flows accumulated, were intruded into progressively higher levels in the volcanic rocks. Thus low down in the volcanic series there is an overwhelming preponderance of intrusive material and towards the top, lavas become increasingly abundant' (Wilson 1959, p. 75).

Ever since Steinmann (1906, 1926) drew attention to the association of serpentinite, pillow lavas, and chert in Alpine ophiolite complexes, they have been a subject of controversy. Much

* Present address: School of Environmental Science, University of East Anglia, Norwich.

of this controversy has been engendered by exposure of these rocks in the Alps where they occur primarily in the Pennide zone (Vuagnat 1963; Burri & Niggli 1945), and where they have been subjected to extensive subsequent metamorphism and tectonism. Outside of the Alps proper, however, ophiolites are recognized widely throughout the Tethyan region (Maxwell & Azzaroli 1963; Trümpy 1960; Gansser 1959; Brunn 1960; Aubouin 1965), and have been reported as well from the circum-Pacific region, e.g. California (Steinmann 1906; Bezore 1969; Hsu 1969), Japan (Miyashiro 1966), Papua (Davies 1969), Macquarie Island (Varne, Gee & Quilty 1969). Where least deformed, these masses characteristically display a consistent sequence, from bottom to top, of magnesian ultramafics, gabbro, diabase, extrusive lava, and deep-sea sediments. Though most masses are allochthonous and many inverted, nearly all preserve the above sequence, regardless of how many zones are preserved.

Three hypotheses for the origin of Alpine ophiolites are currently under consideration, as follows:

(1) That they represent slices of oceanic crust and mantle (Hess 1965; Vine & Hess 1970; deRoever 1957; Moores 1969; Vuagnat 1963).

(2) That they represent diapiric emplacement of partially fused mantle material (Maxwell 1969, 1970; Moores 1969).

(3) That they represent the intrusion into the crust and stratiform crystallization of mafic or ultramafic magma (Smith 1958; Brunn 1956, 1960; Aubouin 1965; Dubertret 1955).

Of the three hypotheses, we favour the first one in the light of presently available evidence. Arguments for and against each hypothesis are complex and involve consideration of individual situations and local details of stratigraphy and regional structure, which are beyond the scope of this article. However, if the first hypothesis is accepted, then the study of ophiolites should reveal a great deal of information about the petrology and structure of oceanic crust.

In this article we present a progress report of a study of a selected ophiolite complex, the Troodos Massif, Cyprus, in an attempt to unravel the processes of oceanic crustal evolution. The Troodos Complex was chosen for this study because of the long-recognized positive gravity anomaly found over the island (Gass & Masson-Smith 1963), and Gass & Masson-Smith's (1963) hypothesis that the Troodos represents an upthrust slice of oceanic crust and mantle. Furthermore, Wilson's work (1959) demonstrated the presence of an apparently unique feature, the 'sheeted' or diabase dyke complex, which seems to imply a mode of formation amounting to sea-floor spreading. Also the Troodos Complex is relatively undeformed and unmetamorphosed; much of it is well mapped; and logistics are easy. It therefore appeared that a restudy would be feasible within the limited amount of time available. Our study would not have been possible without the previous work of the members of the Cyprus Geological Survey Department (Wilson 1959; Bear 1960; Carr & Bear 1960; Gass 1960; Bear & Morel 1960; Bagnall 1960, 1964; Gass & Masson-Smith 1963; Bear 1966; Pantazis 1967, etc.). The observations of Bear & Wilson on the Sheeted Complex and the Plutonic rocks, and of Gass on the Pillow Lava relations were especially valuable. These observations were made before the development of the sea-floor spreading hypothesis by Hess (1962) and Vine & Matthews (1963), but they fit it perfectly. It is clear from the above quotations from Wilson's memoir, for example, that he was conceptually very near to the idea of sea-floor spreading, but did not relate it to the development of the ocean basins.

PHILOSOPHICAL TRANSACTIONS OF THE ROYAL SOCIETY A MATHEMATICAL, PHYSICAL & ENGINEERING SCIENCES

General description of the Troodos Complex

For the purposes of discussion, the Troodos Complex can be divided into three broad units (Wilson 1959; Gass & Masson-Smith 1963; Gass 1967, 1968): Pillow Lava, Sheeted Complex, and Plutonic Complex. It must be emphasized that this division is for descriptive purposes only, and that gradations exist between all units (see figure 1).

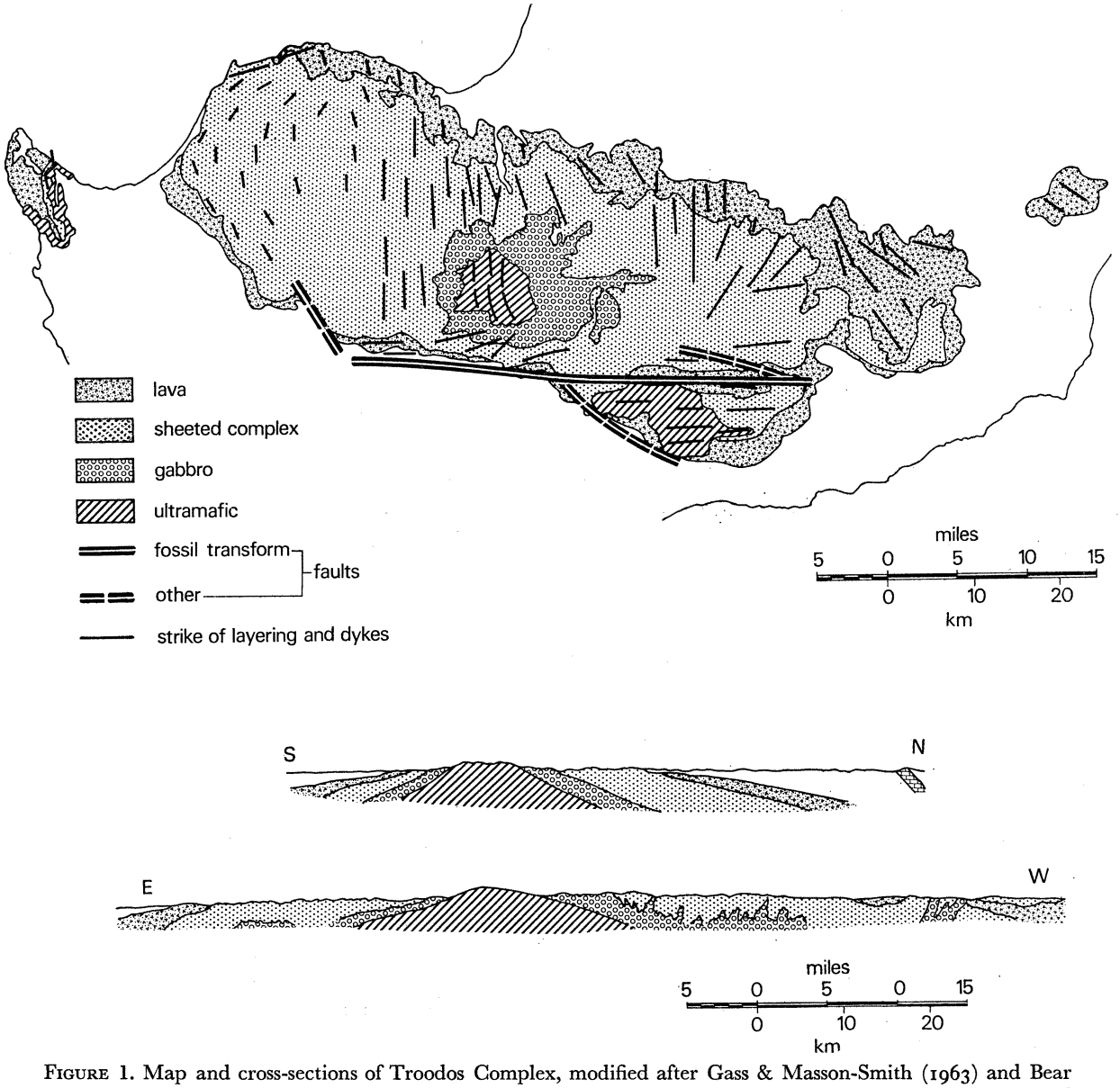

Figure 1. Map and cross-sections of Troodos Complex, modified after Gass & Masson-Smith (1963) and Bear (1965). The Mt Olympus or Troodos ultramafic area is north of the Fossil Transform Fault; the Limassol Forest area borders the Fossil Transform Fault on the south. The western inlier is the Akamas Peninsula, the eastern one is Troulli.

The Plutonic Complex consists of two principal exposures, the Mount Olympus or Troodos area proper, and the Limassol Forest area. These rocks include harzburgite, dunite with accessory chromitite, olivine pyroxenite, gabbro, uralitized gabbro, and albitized quartz diorite.

PHILOSOPHICAL TRANSACTIONS OF THE ROYAL SOCIETY A MATHEMATICAL, PHYSICAL & ENGINEERING SCIENCES

The ultramafic rocks are partly to completely serpentinized. In addition, some remobilization of serpentinite has occurred to the east of Troodos and in the Limassol Forest area. This complex is overlain gradationally by the Sheeted Complex, a massive dyke swarm consisting of 90 to 100 % dykes intruded into a screen of pillow lava in the upper part, and quartz diorite, rare extrusive volcanics, and gabbro in the lower part. The dykes consist of epidosite, keratophyre, and saussuritized dolerite. The pillow lava screens consist primarily of keratophyre, quartz porphyry and epidosite. This complex grades by decreasing abundance of dykes into the pillow lavas above. The Lower Pillow Lavas contain up to 50 % dykes, and are of andesitic basalt, keratophyre and quartz andesite. The Upper Pillow Lavas contain basalt, olivine basalt, and ultrabasic pillow lavas and a few dykes.

Figure 1 also summarizes the local trends of the dyke structure. Generally the dykes trend north–south. In three areas, significant departures from this regional strike are present: in the northwestern part of the island where the dykes strike about N 60° E; in the eastern part of the exposure of the complex, where the dykes strike northwest and northeast, in addition to north–south, in apparently converging trends; and in the south, where marked east–west trends are found associated with east-trending faults which were active during emplacement of the lower units of the complex. At one level within the Sheeted Complex there are 100 % dykes implying, therefore, 100 km of extension in 100 km of exposure. The only possible mechanism which has been proposed to account for such extension is sea-floor spreading.

Our interpretation is that the Troodos Massif as a whole represents a slice of oceanic crust and uppermost mantle, that the harzburgite and dunite of the ultramafic rocks represent depleted mantle, the olivine pyroxenite and gabbro represent intrusive or cumulate magmatic material, that the gabbro and Lower Sheeted Complex (or Diabase) represent seismic layer three of the oceanic crust, and that the upper Sheeted Complex (basal group), Lower Pillow Lavas, and Upper Pillow Lavas represent layer two. Part of the Upper Pillow Lavas represent material added after the main crustal formation.

Upper Pillow Lavas

The Upper Pillow Lavas are discontinuously exposed around the margin of the massif. They consist of pillowed flows and sparse to abundant extrusive breccia, relatively free from intrusives (Wilson 1959; Pantazis 1967; Bagnall 1960). Particularly in the southern portion of the complex, abundant breccias are interbedded with radiolarian manganiferous shales. Most pillow lavas contain olivine phenocrysts, commonly altered to chocolate-brown calcite and are altered to propylitized and zeolite-facies assemblages. Some are quite fresh, however, especially in the northeastern part of the massif (Gass 1960, 1958) and the southern marginal exposures (Wilson 1959; Bear 1960). Figures 2 and 3, plate 5, show typical exposures of pillow lavas and breccia, respectively. Figure 4, plate 5, shows a thin section of a typical olivine basalt. Table 1 presents new and previously published analyses of rocks from the Upper Pillow Lavas. Though variations are present, the analyses show a relatively low SiO_2 and low to high alkalis. Plotted in an alkalis–silica diagram (figure 5), these rocks show a tendency towards the alkaline side, though no mineralogy on pyroxenes has yet been done to test the validity of this trend. However, there is a general compositional consistency between altered and unaltered rocks. The Upper Pillow Lavas apparently overstep onto rocks of the Sheeted Complex in the north-central portion of the massif (Wilson 1959; Carr & Bear 1960; Gass 1960), but apparently no break can be found in the northeast (Gass 1960). In the south, however, Upper Pillow Lavas overlie with marked

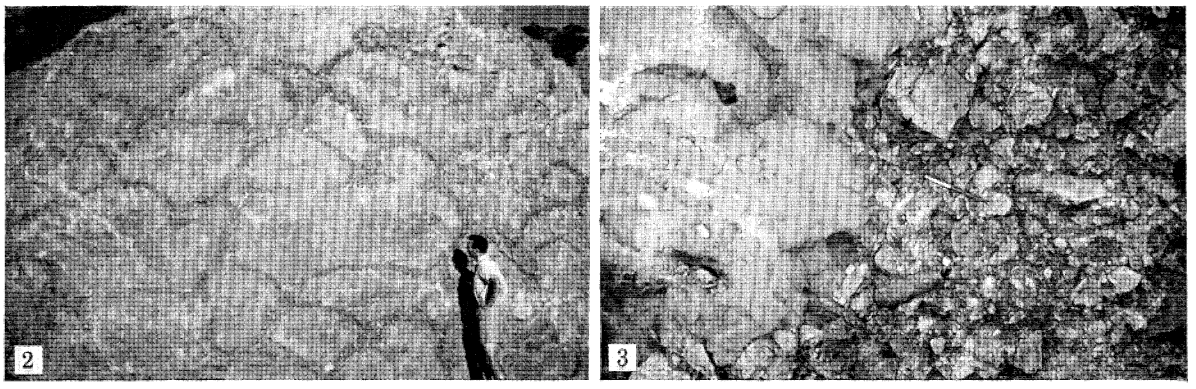

FIGURE 2. Exposure of Upper Pillow Lavas. Note intrusive-free exposure, hyaloclastic matrices between pillows, veining of calcite and analcite. Northwest margin of the massif.

FIGURE 3. Photo of breccia in Upper Pillow Lava, near southeastern margin of massif.

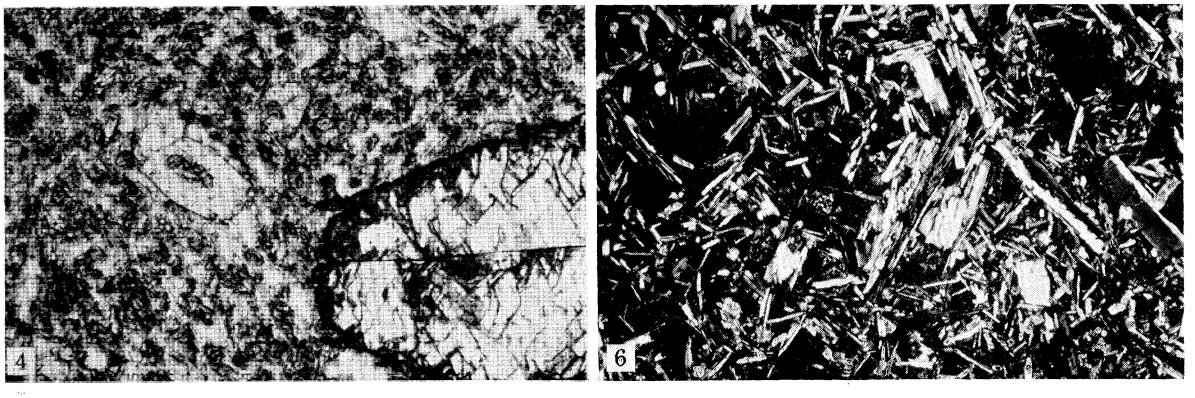

FIGURE 4. Photomicrograph of Upper Pillow Lava rock. Phenocrysts are calcite replacements of olivine in microcrystalline to glassy altered groundmass. Plain light, max. dimension 1.6 mm.

FIGURE 6. Photomicrograph of dyke intrusive into Lower Pillow Lavas. Plagioclase and augite microphenocrysts in a seriate groundmass of plagioclase and alteration products. Crossed Nicols, max. dimension 3.2 mm.

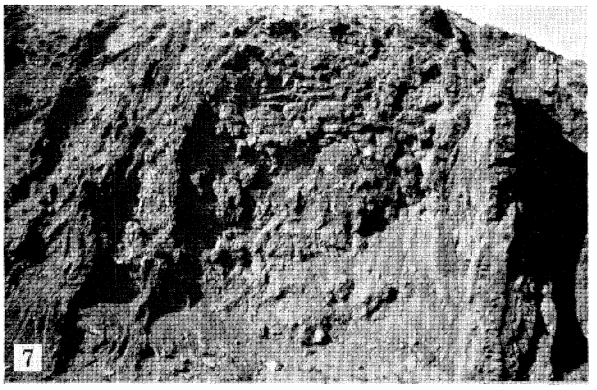

FIGURE 7. Stream exposure of Lower Pillow Lavas, near contact with Sheeted Complex. Note composite dykes intruding flat-lying pillow lavas. Area below distinctive pillow structure is brecciated pillow lavas intruded by numerous small irregular sills.

(*Facing p.* 446)

FIGURE 11. Photo of Sheeted Diabase showing typical aspect. Max. width of photo approx. 1.5 km.

FIGURE 15. Photomicrograph of olivine gabbro, labradorite, olivine, augite, and iron ore. Crossed Nicols, max. dimension 3.2 mm.

FIGURE 16. Thin section of cumulate-textured olivine pyroxenite. Subhedral olivine, anhedral, twinned, poikilitic augite. Crossed Nicols, max. dimension 3.2 mm.

FIGURE 17. Foliated harzburgite. Fabric marked by planar orientation of olivine grains and enstatite layers. Troodos ultramafic area.

FIGURE 18. Isoclinal fold in dunite and chromitite. Troodos ultramafic area.

PHILOSOPHICAL TRANSACTIONS OF THE ROYAL SOCIETY A MATHEMATICAL, PHYSICAL & ENGINEERING SCIENCES

TABLE 1. CHEMICAL ANALYSES, UPPER PILLOW LAVAS

	(a)	(b)	(c)	(d)	(e)	(f)	(g)	(h)	(i)	(j)	(k)	(l)	(m)	(n)	(o)
SiO_2	45.73	43.00	42.38	43.39	45.04	49.86	47.60	47.43	42.11	48.00	46.5	45.5	46.4	50.8	49.7
Al_2O_3	15.42	4.64	4.97	12.83	7.13	11.92	11.78	14.81	6.59	14.75	14.4	12.1	14.6	15.2	15.6
Fe_2O_3	5.68	2.42	3.15	4.90	3.13	3.35	2.96	6.19	3.62	6.33	9.2	8.5	7.9	8.2	7.8
FeO	2.20	6.47	5.25	2.10	5.43	4.94	6.70	2.49	5.38	1.61					
MgO	8.91	33.45	31.72	8.06	26.16	10.17	14.08	3.44	30.00	7.12	8.2	7.1	10.8	9.4	8.9
CaO	5.84	3.99	4.66	11.84	5.56	9.65	7.91	14.32	3.39	8.50	11.7	11.7	7.8	7.8	2.3
Na_2O	2.63	0.25	0.40	1.04	0.77	1.70	1.58	2.43	0.25	0.82	4.2	1.7	4.2	1.8	0.08
K_2O	1.90	0.05	0.12	3.25	0.06	0.37	0.75	1.43	0.17	4.85	0.04	2.1	0.8	2.7	0.09
H_2O^+	3.81	3.83	4.18	3.16	3.81	4.49	3.62	1.49	6.05	3.33	—	—	—	—	—
H_2O^-	5.92	1.22	1.52	3.84	1.89	3.07	1.44	0.68	1.89	2.53	—	—	—	—	—
CO_2	1.12	—	0.86	4.85	0.07	—	0.04	4.41	—	2.19	—	—	—	—	—
TiO_2	0.73	0.18	0.28	0.49	0.36	0.53	1.34	0.64	0.23	0.34	0.8	0.38	0.64	0.54	0.7
P_2O_5	0.09	—	0.05	0.08	0.12	0.06	0.02	0.09	0.05	0.06	—	—	—	—	—
MnO	0.17	0.15	0.14	0.11	0.14	0.14	0.15	0.10	0.16	0.08	—	0.08	0.12	0.08	0.15
Cr_2O_3	0.04	0.51	0.39	—	0.32	0.11	0.09	—	0.28	0.02	0.21	—	—	—	—
NiO	—	—	—	—	—	—	0.05	—	0.12	S 0.05	—	—	—	—	—
	100.19	100.16	100.06	99.94	99.99	100.36	100.11	99.95	100.29	100.58					

Remarks:

(*a*) Basalt, Kambia Village: Bear (1960), table III, Analysis 1574, p. 58.

(*b*) Ultrabasic pillow lava, 1.2 km SW of Margi: Gass (1960), table III, Analysis 1370, p. 83.

(*c*) Ultrabasic lava, 1.2 km west of Margi: Bear (1961), Analysis 1, p. 11.

(*d*) Mugearite, Alikos River, 800 m west of Margi: Bear (1961), Analysis 2, p. 11.

(*e*) Ultrabasic lava, 2 km south of Margi: Bear (1961), Analysis 3, p. 11.

(*f*) Limburgite, 800 m west of Margi: Bear (1961), Analysis 5, p. 11.

(*g*) Olivine norite intrusive, east of Agrokipia: Bear (1960), table IV, Analysis 1564, p. 77.

(*h*) Quartz gabbro intrusive, east of Agrokipia: Bear (1960), table IV, Analysis 1566, p. 77.

(*i*) Peridotite plug, 800 m SW of Margi: Gass (1960), table III, Analysis 1374, p. 83.

(*j*) Trachybasalt dyke, 1.6 km east of Vouni: Wilson (1959), table I, Analysis 684, p. 69.

(*k*) Altered olivine basalt, near Troulli: new XRF analysis, sample 19 D.

(*l*) Altered dolerite dyke, near Kellaki: new XRF analysis, sample 23F.

(*m*) Altered olivine basalt, near Malounda: new XRF analysis, sample 30A.

(*n*) Altered dolerite dyke, near Malounda: new XRF analysis, sample 30B.

(*o*) Basalt, core from drill hole, near Koutraphas, North-central margin of Complex: new XRF analysis, sample UPL–K.

unconformity faulted exposures of Sheeted Complex and Lower Pillow Lavas. These relations taken together indicate that a slight to substantial unconformity separates Lower and Upper Pillow Lavas.

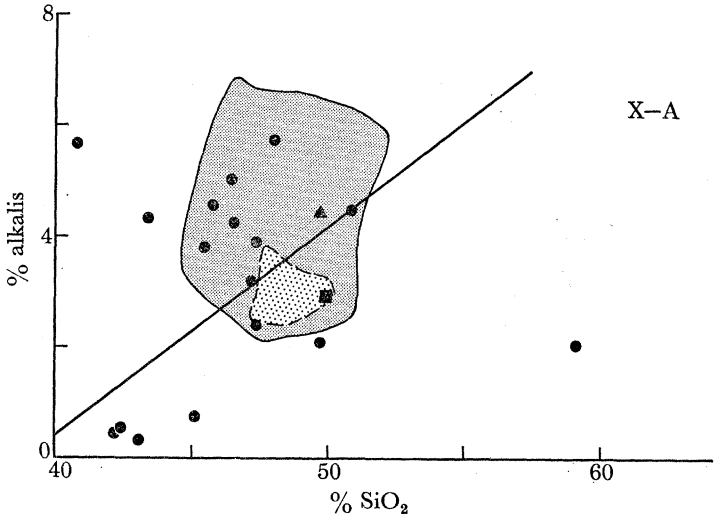

FIGURE 5. Alkalis–silica diagram for Upper Pillow Lava rocks. Heavy line is Hawaii alkalic-tholeiitic division line, as defined by MacDonald & Katsura (1964); fine-stippled area is field of analyses from mid-Atlantic Ridge at 45° N (Aumento & Loncarevic 1969; Aumento 1968). Heavy pattern field of analyses reported by Muir & Tilley (1964, 1966). Mid-Atlantic diorite (– A) is from Aumento (1969). Average spilite (▲) from Poldervaart (1955), average oceanic tholeiite (■) from Engel *et al.* (1965). ●, flows and intrusives.

Lower Pillow Lavas

Lower Pillow Lavas characteristically display plagioclase and pyroxene phenocrysts in a groundmass of altered plagioclase and iron ore (see figure 6, plate 5). Albitization and celadonite alteration are common, as are quartz and chalcedony amygdules. Characteristic also is the presence of 10 to 50 % dykes. showing chilled margins and multiple intrusive nature (see figure 7, plate 5). Chilled margins are also common in pillows, in contrast to similar exposures in the Upper Pillow Lavas. The contact between the Lower Pillow Lavas and the Basal Group (the upper unit of the Sheeted Complex) is marked by intrusion of sills, a sharp increase of dyke density in some areas (Gass 1960), gradual increase in other areas (Bear 1960; Wilson 1959), and local relief of up to 2 km (Gass 1960. pl. 1). The sharp increase in dyke density and relief on the contact in the eastern part of the area has prompted Gass (1960, 1967, 1968) to postulate an unconformity between Lower Pillow Lavas and Basal Group. In view of the transitional nature of the contact elsewhere, however, and the lack of an erosional surface and intercalated sediments, we prefer to interpret this apparent disconformity as resulting from relative variations in spreading rate against magma supply as discussed below.

Chemically, as well as petrographically, the Lower Pillow Lavas differ somewhat from the Uppers. Table 2 presents available chemical analyses of rocks from the Lower Pillow Lavas. It will be seen that they are often characterized by high silica, low potash, and variable amounts of other elements. There is, however, a consistent grouping of K_2O contents around 0.25 % as shown in figure 8, in contrast to the greater spread of Upper Pillow Lava values. Figure 9 shows a plot of Lower Pillow Lava rocks on a silica–alkalis diagram. Compared with the Upper Pillow Lavas (figure 6) most rocks are lower in alkalis, higher in SiO_2 and show a general increase of alkalis with increasing SiO_2 content.

PHILOSOPHICAL TRANSACTIONS OF THE ROYAL SOCIETY A MATHEMATICAL, PHYSICAL & ENGINEERING SCIENCES

TABLE 2. CHEMICAL ANALYSES, LOWER PILLOW LAVAS

	(a)	(b)	(c)	(d)	(e)	(f)	(g)	(h)	(i)	(j)	(k)	(l)	(m)	(n)	(o)	(p)	(q)	(r)	(s)	(t)	(u)	(v)	(w)	(x)
SiO_2	51.71	65.22	50.67	52.01	66.18	63.32	46.6	47.8	51.6	53.2	52.8	56.1	69.9	50.9	59.6	41.0	53.6	53.8	63.2	74.3	48.4	55.7	49.7	48.0
Al_2O_3	14.70	12.71	15.61	14.77	12.78	15.68	15.2	15.9	15.4	15.3	14.4	14.4	13.0	15.2	13.6	15.1	15.8	14.6	13.1	10.5	17.6	15.2	16.6	15.2
Fe_2O_3	1.86	2.84	8.15	4.32	1.37	7.37	10.9	10.9	10.9	8.5	8.4	11.5	5.5	13.5	10.5	8.4	10.3	11.1	8.4	3.6	13.2	10.5	13.5	13.2
FeO	6.34	4.72	2.67	5.83	3.52																			
MgO	7.55	0.64	2.21	6.54	0.72	1.39	6.6	8.4	7.5	4.8	7.6	5.8	1.8	5.8	5.1	6.3	4.1	4.4	4.5	2.5	3.4	4.4	3.5	6.0
CaO	10.74	3.81	11.21	4.00	2.98	5.04	9.8	9.2	8.7	11.2	9.9	5.7	4.8	8.6	5.6	11.0	9.3	9.6	4.9	2.0	6.8	7.8	8.4	6.9
Na_2O	1.88	4.58	3.05	2.08	4.03	2.55	2.2	1.5	2.3	2.2	1.8	3.0	4.0	2.6	3.0	5.4	2.8	2.4	3.6	4.5	3.4	3.4	3.3	3.1
K_2O	0.25	0.60	0.36	2.48	1.60	1.69	0.20	0.50	0.37	0.22	0.19	0.20	0.22	0.16	0.19	1.0	0.57	0.60	0.20	0.22	1.69	0.20	1.05	0.34
H_2O^+	3.70	3.63	0.81	3.86	4.41	—	—	—	—	—	—	—	—	—	—	—	—	—	—	—	—	—	—	—
H_2O^-	0.82	0.39	1.31	2.23	2.39	1.65	—	—	—	—	—	—	—	—	—	—	—	—	—	—	—	—	—	—
CO_2	—	0.04	2.06	0.44	—	—	—	—	—	—	—	—	—	—	—	—	—	—	—	—	—	—	—	—
TiO_2	0.48	0.55	1.01	1.01	0.34	1.15	0.98	0.86	0.84	0.56	0.52	1.15	1.12	1.32	1.45	0.52	1.0	0.87	0.66	0.29	1.58	1.36	1.30	1.47
P_2O_5	0.06	0.19	0.11	0.10	0.09	—	—	—	—	—	—	—	—	—	—	—	—	—	—	—	—	—	—	—
MnO	0.15	0.18	0.35	0.27	0.13	0.03	0.25	0.10	0.11	0.10	0.11	0.10	0.10	0.16	0.16	0.24	0.16	0.14	0.07	0.07	0.16	0.14	0.16	0.24
Cr_2O_3	—	—	S 1.17	—	—	—	—	—	—	—	—	—	—	—	—	—	—	—	—	—	—	—	—	—
	100.24	100.10	100.75	99.94	100.54	99.87																		

Remarks:

(*a*) Augitite dyke, south of Kambia: Bear (1960), table III, Analysis 1767, p. 58.
(*b*) Dacite glass, Xyliatos: Carr & Bear (1960), Analysis 1063, p. 35.
(*c*) Quartz basalt dyke, 1.6 km SW of Skouriotissa: Wilson (1959), table I, Analysis 188, p. 69.
(*d*) Andesite, Mitsero: Bear (1960), table III, Analysis 1569, p. 58.
(*e*) Glassy dacite, Kokkinoyia: Bear (1960), table III, Analysis 1265, p. 58.
(*f*) Andesite, 2.4 km south of Kambia: Bear (1960), table III, Analysis 1623, p. 58.
(*g*) Vesicular andesite, south of Troulli: new XRF analysis, sample 21D.
(*h*) Altered basalt, Malounda: new XRF analysis, sample 30E.
(*i*) Interior of altered basalt pillow, Malounda: new XRF analysis, sample 30G.
(*j*) Altered basalt, base of flow, Malounda: new XRF analysis, sample 30J.
(*k*) Altered basalt dyke margin, Malounda: new XRF analysis, sample 30F.
(*l*) Altered basaltic dyke, Klirou: new XRF analysis, sample 32M.
(*m*) Altered glassy dyke, Klirou: new XRF analysis, sample 32P.
(*n*) Altered basaltic pillow margin, Klirou: new XRF analysis, sample 32N.
(*o*) Altered basaltic dyke: new XRF analysis, sample 32R.
(*p*) Altered pillow lava, NW of Mathiati: new XRF analysis, sample 8A.
(*q*) Fresh pillow lava, near Karpedhes: new XRF analysis, sample 12R.
(*r*) Altered basalt sill, SE of Mathiati: new XRF analysis, sample 17P.
(*s*) Altered quartz dolerite dyke, SE of Mathiati: new XRF analysis, sample 17S.
(*t*) Altered dacite, Troulli: new XRF analysis, sample 19B.
(*u*) Altered pillow lava, Karpedhes: new XRF analysis, sample 12C.
(*v*) Altered basaltic intrusive, Karpedhes: new XRF analysis, sample 12Y.
(*w*) Altered dolerite, Troulli: new XRF analysis, sample 20C.
(*x*) Drill core near Analiondas, altered basalt: new XRF analysis, sample AN270.

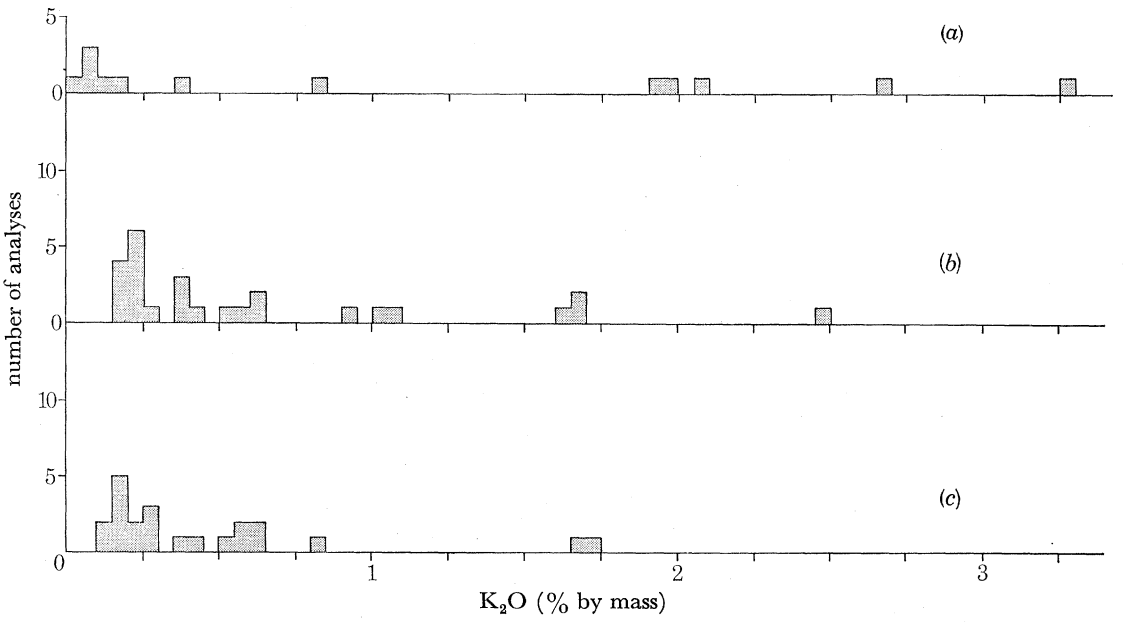

FIGURE 8. Plot of K_2O content against number of analyses for (*a*) Upper Pillow Lava, (*b*) Lower Pillow Lava and (*c*) Sheeted Complex.

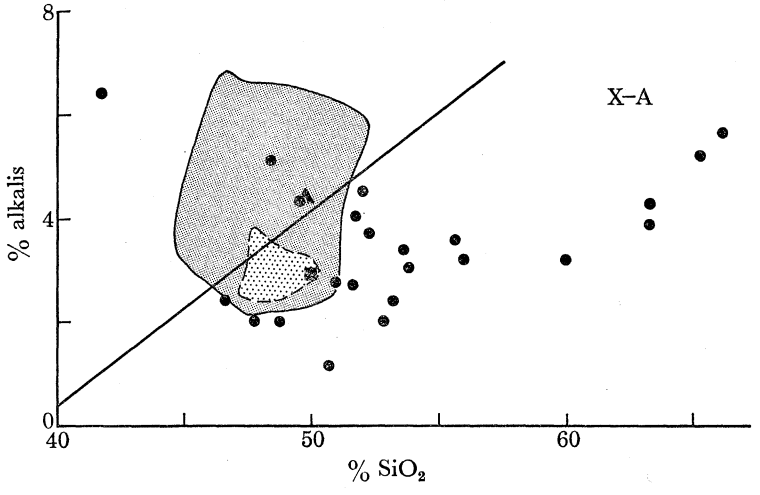

FIGURE 9. Silica-alkalis plot for flows and intrusives of Lower Pillow Lavas. See figure 5 for explanation of symbols.

Sheeted Complex

The Sheeted Intrusive Complex has been subdivided by the Cyprus Geological Survey Department into two units depending upon the type of screens present. The Basal Group consists of 90 to 100 % dykes in screens of pillow lava. Figure 10, adapted from Wilson, shows several typical sections through this unit. Pillow lavas of this unit include greenstones, keratophyres, and andesites, similar to those of the Lower Pillow Lavas, but which have been subjected to more pronounced greenschist metamorphism. Dykes in this unit include epidosites, keratophyres and greenstones. The distinction between this unit and the underlying diabase has been made on the basis of the presence or absence of pillow lava screens. Consequently the contacts are subjective and approximate.

Rocks assigned to the Diabase include dyke swarms composed of 100 % dykes, many of which show little or no chilled margins. In addition, much of the massif mapped as Diabase includes diabase intruded into screens of gabbro, quartz-diorite, and unpillowed amygdaloidal, porphyritic (presumably extrusive) rock. Figure 11, plate 6, shows a typical exposure of sheeted Diabase. Particularly apparent is the vertically dipping 'grain' extending the width of the photograph.

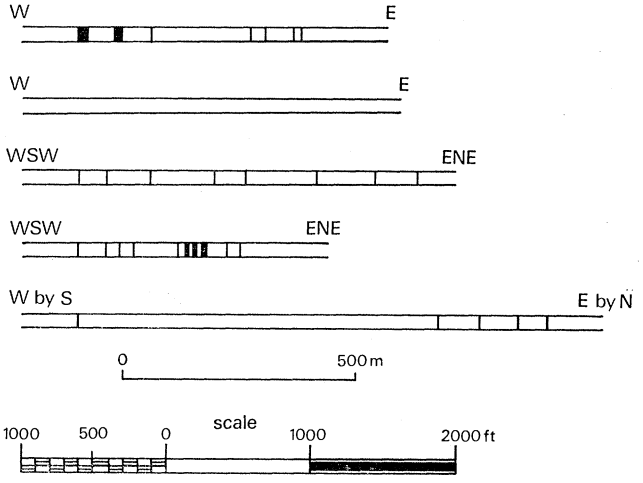

FIGURE 10. Representative cross-sections of Basal Group exposures, adapted from Wilson (1959). Black vertical lines are screens of pillow lava. White areas are dyke complexes.

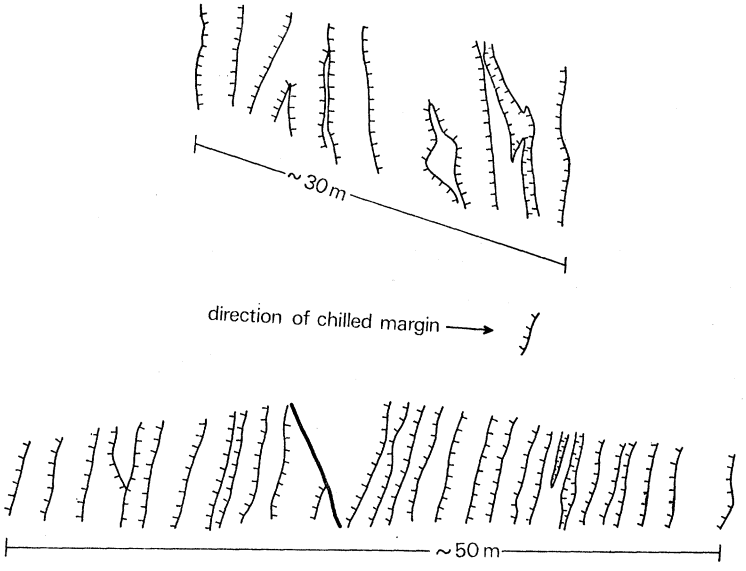

FIGURE 12. Representative cross-sections of Sheeted Complex.

The multiple intrusive nature of the dykes is illustrated in figures 7 and 11. In figure 7 the 'ribs' standing in relief represent individual chilled margins of a single dyke. Apparently the process has been that one dyke is intruded and has its margins chilled against the wall rock. The next dyke then intrudes up the middle of the previous one, and in turn forms chilled margins, then the next one repeats, and so on. This process apparently has been operative in the Sheeted Complex as well, but much more extensively, so that in a single exposure one can

rarely see the two sides of a multiple intrusive dyke. Figure 12 shows two sketches of road cuts illustrating the preponderance of one-sided chilled margins of such an exposure. These relations indicate that the main process of formation was one of multiple intrusion of small volumes of magma, and that enough time was available for the previous rock to cool sufficiently for the succeeding pulse to be chilled.

Although most dykes are oriented so that their original dip must have been vertical, in some places conjugate sets of cross-cutting dykes are present within the same exposure. We interpret these conjugate dykes to indicate variations in extension against magma injection, as discussed below. Some kilometre-sized areas of consistent moderate to steep dip are adjacent to similarly sized areas of opposite dip. These areas of opposing dip may represent conjugate sets on a larger scale or tilted blocks originally of the same dip.

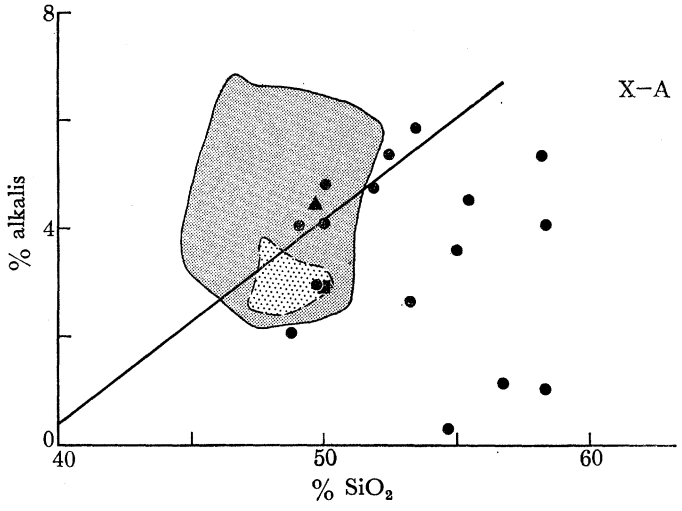

FIGURE 13. Silica-alkalis plot for rocks of Sheeted Complex. See figure 5 for explanation of symbols.

Though the strike of the intrusives in a given local area is generally uniform, in a few places sharp changes of almost 90° are present; this is in addition to the more regional changes present in the northwestern, southern, and eastern portions of the massif. Remanent magnetization directions suggest that these changes in strike are a function of original attitude at time of intrusion, rather than any case of tectonic rotation as implied by Bagnall (1964).

Available chemical analyses of rocks from the Sheeted Complex (table 3) display similarities with the Lower Pillow Lavas in generally moderate to high SiO_2 and low K_2O (see also figure 8). The silica–alkalis plot of these rocks (figure 13) places them generally in the same areas as the Lower Pillow Lavas (see figure 9).

The contact of the Diabase with the underlying Plutonic rocks is complex. Although much of the lower Diabase consists of diabase dykes intrusive into screens of gabbro and quartz diorite, intrusive contacts of gabbro and quartz diorite into Diabase are also present. Also, much rock mapped as gabbro and quartz diorite actually has a considerable number of dykes. Hence the contact between the plutonic and diabasic rocks is irregularly gradational and apparently represents a zone of multiple intrusion.

PHILOSOPHICAL TRANSACTIONS OF THE ROYAL SOCIETY A MATHEMATICAL, PHYSICAL & ENGINEERING SCIENCES

TABLE 3. CHEMICAL ANALYSES, SHEETED COMPLEX

	(a)	(b)	(c)	(d)	(e)	(f)	(g)	(h)	(i)	(j)	(k)	(l)	(m)	(n)	(o)	(p)	(q)	(r)	(s)	(t)
SiO_2	51.78	58.36	50.07	53.40	78.27	77.04	49.10	54.98	58.31	54.70	52.67	56.36	49.84	58.2	53.2	53.4	49.5	74.6	48.7	51.6
Al_2O_3	14.10	14.08	15.54	15.40	11.43	10.95	15.60	14.17	13.73	14.86	15.28	16.92	17.87	14.4	16.0	15.3	14.9	11.8	15.5	15.2
Fe_2O_3	3.88	5.92	2.08	10.46	1.44	2.14	2.08	7.14	3.78	5.88	3.68	11.68	9.98	9.6	9.1	10.1	11.8	4.4	9.3	10.4
FeO	5.15	1.80	8.06		0.14	0.79	5.04	4.95	5.53	4.21	6.02									
MgO	8.07	2.91	8.78	5.12	0.57	0.70	10.42	4.69	4.63	4.67	5.51	3.68	6.48	4.6	5.2	7.2	8.4	3.7	6.1	7.2
CaO	7.23	12.74	4.50	7.37	0.92	1.86	7.58	4.51	5.34	10.89	6.80	7.45	9.35	4.1	11.7	3.4	8.7	2.3	13.3	6.1
Na_2O	4.50	0.75	4.43	3.87	4.70	4.63	2.38	1.83	3.45	0.16	4.62	1.96	2.50	5.0	2.0	5.6	3.6	4.8	1.6	4.2
K_2O	0.23	0.25	0.35	0.60	0.53	0.18	1.65	1.73	0.59	0.13	0.82	0.18	0.42	0.78	0.63	0.20	0.17	0.16	0.44	0.61
H_2O^+	2.73	1.32	4.14	2.24	1.39	0.79	4.22	2.93	2.14	2.60	2.83	1.30	2.94	—	—	—	—	—	—	—
H_2O^-	1.27	0.79	0.96	—	0.53	0.26	1.64	1.99	0.90	1.10	0.62			—	—	—	—	—	—	—
Co_2	0.14	—	0.26	—	—	—	—	—	—	0.17	0.12	—	—	—	—	—	—	—	—	—
TiO_2	0.54	0.58	0.48	0.95	0.25	0.20	0.30	1.11	1.30	0.68	0.93	0.35	0.40	1.02	0.54	0.53	1.07	0.21	0.55	0.66
P_2O_5	0.08	0.03	0.09	—	0.05	0.05	0.04	0.10	0.11	0.06	0.07	—	—	—	—	—	—	—	—	—
Cr_2O_3	—	—	—	—	—	—	—	—	—	—	—	—	—	—	—	—	—	—	—	—
MnO	0.26	0.20	0.20	0.12	0.03	0.05	0.18	0.18	0.25	0.26	0.16	0.16	0.23	0.10	0.13	0.14	0.2	0.07	0.13	0.19
NiO	—	—	—	—	—	—	—	—	—	—	—	—	—							
F	—	—	0.07	—	—	—	—	S 0.06	—	S 0.06	—	—	—							
	99.96	99.73	1000.01	99.83	100.25	99.64	100.23	100.37	100.06	100.03	100.13	100.04	100.01							

Remarks:

(*a*) Andesite pillow lava, Basal Group, 2.4 km north of Pharmakas: Bear (1960), table II, Analysis 1582, p. 51.

(*b*) Epidosite pillow lava, Basal Group, 2.4 km SW of Kalokhorio: Bear (1960), table II, Analysis 1583, p. 51.

(*c*) Greenstone (chlorite-actinolite) pillow lava, Basal Group, Kalokhorio: Bear (1960), table II, Analysis 1790, p. 71.

(*d*) Microdiorite intrusive: Bear (1960), table II, Analysis 1775, p. 51.

(*e*) Quartz-albite microporphyry. 1.6 km NE or Pyrga: Gass (1960), table III, Analysis 1366, p. 83.

(*f*) Quartz-albite porphyry, 800 m north of Psevda: Gass (1960), table III, Analysis 1381, p. 83.

(*g*) Serpentinized microgabbro, 1.6 km north of Mosphiloti: Gass (1960), table III, Analysis 1379, p. 83.

(*h*) Quartz diabase dyke, Basal Group, 1.6 km SW of Kato Vlaso: Wilson (1959), table I, Analysis 149, p. 69.

(*i*) Quartz diabase, Kykko: Wilson (1969), table I, Analysis 662, p. 69.

(*j*) Epidosite, Lefka-Pedoulas Road: Wilson (1959), table IV, Analysis 667, p. 98.

(*k*) Microdiorite, Gourrie: Bear & Morel (1960), table II, Analysis 2808, p. 30.

(*l*) Microgabbro, Ayios Theodoros: Bear & Morel (1960), table II, Analysis 2871, p. 30.

(*m*) Microgabbro, Ayios Theodoros: Bear & Morel (1960), table II, Analysis 2872, p. 30.

(*n*) Altered dolerite, north of Kellaki: new XRF analysis, sample 25C.

(*o*) Altered dolerite, south of Troulli: new XRF analysis, sample 21F.

(*p*) Altered dolerite, south of Melini: new XRF analysis, sample 29E.

(*q*) Altered dolerite, south of Melini: new XRF analysis, sample 29A.

(*r*) Altered dolerite, Basal Group, west of Lefkara: new XRF analysis, sample 33A.

(*s*) Altered dolerite, south of Troulli: new XRF analysis, sample 21B.

(*t*) Altered microgabbro, south of Lefka: new XRF analysis, sample 120B.

Plutonic rocks

Rocks of the Plutonic Complex include 'granophyre' or quartz diorite, uralitized gabbro, norite, olivine gabbro, troctolite, poikilitic olivine pyroxenite, dunite with accessory chromitite and harzburgite or 'enstatite olivinite' (see figure 14).

Quartz diorite is present as screens in Diabase, as 'sheeted' and 'unsheeted' bodies intrusive into Diabase, and as residual segregations in gabbro. Most of these rocks are medium to coarse grained, containing abundant quartz, zoned plagioclase, and chlorite alteration after mafics. Chemical analyses of these rocks exhibit very high SiO_2 and low K_2O contents (see table 4). Table 4 also includes an analysis of a Mid-Atlantic quartz diorite (Aumento 1969) for comparison. Zoned feldspars have andesine cores and albitic rims.

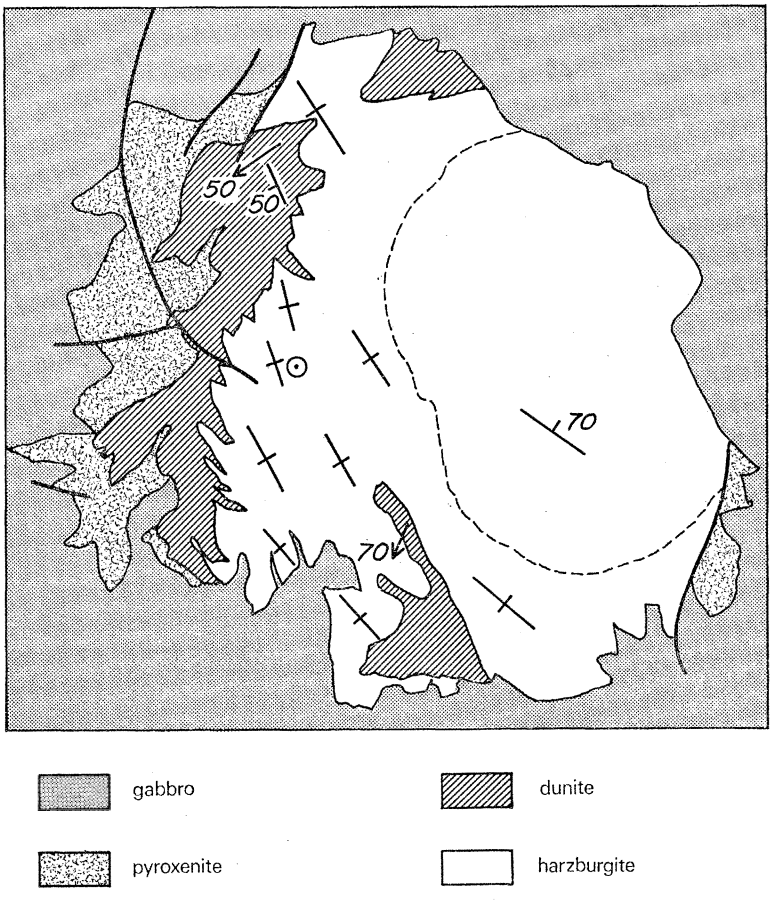

FIGURE 14. Generalized map of Troodos ultramafic area, showing attitudes of foliation and lineations. Dashed line in harzburgite outlines remobilized serpentinite plug.

Gabbroic rocks are found in two main areas—extensively surrounding the Troodos ultramafic mass, and in limited outcrops in the Limassol Forest area. In the former area, uralitized gabbro, norite, olivine gabbro, and troctolite are present. Uralitized gabbro is gradational into both quartz diorite and norite, and includes rocks in which amphibole has clearly altered from pyroxene, as well as rocks where it apparently represents a primary phase. The former have heavily altered calcic plagioclases surrounded by albitic rims, the latter have fresh calcic plagioclases with albitic rims. Norite contains two pyroxenes and plagioclase, and commonly grades into olivine-bearing rocks. Textures tend to be anhedral granular with reaction rims of pyroxene

PHILOSOPHICAL TRANSACTIONS OF THE ROYAL SOCIETY A MATHEMATICAL, PHYSICAL & ENGINEERING SCIENCES

TABLE 4. QUARTZ DIORITES, ANORTHOSITES, AND GABBROS

	(a)	(b)	(c)	(d)	(e)	(f)	(g)	(h)	(i)	(j)	(k)	(l)	(m)	(n)
SiO	73.06	76.58	73.31	76.85	64.54	46.07	49.10	54.76	51.20	49.9	48.16	45.56	39.92	56.43
Al_2O_3	12.30	11.61	13.40	12.36	14.03	22.21	18.20	15.31	15.80	5.2	9.35	29.90	26.00	26.10
Fe_2O_3	2.32	2.06	5.59	0.76	4.12	0.87	1.18	2.06	6.84	6.8	9.58	2.00	1.59	0.51
FeO	2.23	0.54	—	0.50	3.38	2.74	4.23	5.81	—	—	—	—	—	0.63
MgO	0.65	0.60	0.71	0.63	6.16	8.82	10.56	7.01	8.40	19.8	17.18	4.90	5.00	0.92
CaO	3.56	4.10	1.35	1.84	3.52	17.48	15.64	10.33	11.73	16.3	13.60	17.07	19.47	8.34
Na_2O	3.90	3.36	5.00	5.60	5.40	0.68	0.38	2.43	3.81	0.4	0.50	0.25	0.15	6.36
K_2O	0.18	0.18	tr	0.25	0.58	0.11	0.08	0.24	0.43	0.01	tr	tr	0.21	0.07
H_2O^+	1.09	0.97	0.54	0.54	0.52	1.03	0.77	1.49	—	—	1.41	1.50	7.50	0.23
H_2O^-	0.52	0.31	—	0.41	1.29	0.23	0.15	0.29	—	—	—	—	—	0.01
CO_2	—	—	—	0.02	0.07	—	—	—	—	—	—	—	—	—
TiO_2	0.28	0.19	0.10	0.29	0.92	0.08	0.12	0.55	0.29	0.19	tr	tr	0.35	0.18
P_2O_5	0.07	0.10	—	0.03	0.22	0.05	0.06	0.07	—	—	—	—	—	tr
S	—	—	—	—	—	0.09	—	—	—	—	—	—	—	—
Cr_2O_3	—	—	—	—	—	0.04	—	—	—	—	—	—	—	—
MnO	0.05	0.02	0.10	0.01	0.10	0.08	0.13	0.16	0.12	0.12	0.27	tr	tr	0.01
	100.21	100.62	100.10	100.09	99.85	100.45	100.60	100.51	—	—	100.05	100.08	100.29	99.79

Remarks:

(*a*) Granophyric hornblende-trondhjemite, SE Troodos–Limassol–Saittas Road: Wilson (1959), table IV, Analysis 1157, p. 98.

(*b*) Granophyric epidote trondjemite, Lefka–Pedoulas Road: Wilson (1959), table IV, Analysis 1153, p. 98.

(*c*) Quartz porphyry host rock, Zoopiyi: Bear & Morel (1960), table I, Analysis 2825, p. 28.

(*d*) Trondjemite, Gourrie: Bear (1960), table IV, Analysis 1577, p. 77.

(*e*) Tonalite, Gourrie: Bear (1960), table IV, Analysis 1576, p. 77.

(*f*) Gabbro-Platres end of old road to Troodos: Wilson (1959), table III, Analysis 124, p. 90.

(*g*) Hypersthene-gabbro, near milepost 39, Kakopetria–Troodos Road: Wilson (1959), table III, Analysis 1150, p. 90.

(*h*) Uralite gabbro, near milepost 47, Lefka–Pedhoulas Road: Wilson (1959), table III, Analysis 1158, p. 90.

(*i*) Gabbro, Limassol Forest area: Pantazis (1967), table V, Analysis 8612, p. 89.

(*j*) Olivine gabbro, Limassol Forest area, about 3.2 km south of Kellaki: new XRF Analysis, sample 24P.

(*k*) Olivine gabbro, east of Khandria: Bear & Morel (1960), table III, Analysis 2870, p. 41.

(*l*) Fine grained anorthosite, east of Louvaras: Bear & Morel (1960), table III, Analysis 2873, p. 41.

(*m*) Coarse-grained anorthosite, N.E of Apsiou: Bear & Morel (1960), table III, Analysis 2874, p. 41.

(*n*) Anorthosite, Central Indian ridge: Engel & Fisher (1969), table 3, p. 1138.

and/or amphibole around olivine (see figure 15, plate 6). Generally minerals are quite fresh, and little or no zoning is present in the plagioclase.

In the Limassol Forest area, gabbros and associated mafic rocks are not abundant, but occur as layered to massive rocks apparently overlying serpentinized peridotite. Subsequent remobilization of the latter, however, makes it difficult to determine the exact original relationships. Noteworthy in this area are the presence of three small bodies of anorthosite within the gabbro (Bear 1960, pp. 40–42). Bear describes an intimate interlayering of anorthosite and gabbro and uncommon dyke-like anorthosite masses. He also reports the presence of protoclastic texture. Table 4 presents an analysis of two of these rocks, together with one from the Indian Ocean (Engel & Fisher 1969) for comparison. Such a comparison is of doubtful validity, however, because the chemical composition strongly depends on modal percentages of minerals present.

TABLE 5. CHEMICAL ANALYSES, ULTRAMAFIC ROCKS

	(*a*)	(*b*)	(*c*)	(*d*)	(*e*)	(*f*)
SiO_2	46.27	39.54	33.72	37.68	42.93	38.59
Al_2O_3	2.31	5.15	0.51	0.56	4.43	1.97
Fe_2O_3	2.74	3.48	4.06	4.80	4.13	8.51
FeO	3.76	4.39	3.21	2.88	5.24	2.00
MgO	29.24	32.71	41.82	39.32	28.30	33.24
CaO	12.12	4.06	0.15	0.54	7.30	1.28
Na_2O	0.15	0.14	—	—	0.15	0.04
K_2O	0.07	0.09	—	—	0.05	0.05
H_2O^+	2.84	8.81	14.97	12.65	6.24	13.27
H_2O^-	0.28	0.85	0.93	0.89	—	—
Co_2	—	—	0.59	0.36	0.10	0.10
TiO_2	0.06	0.03	—	—	0.11	0.07
P_2O_5	0.13	0.20	0.04	0.04	0.03	0.03
S	—	0.18	0.02	0.08	—	—
Cr_2O_3	0.44	0.36	0.11	0.24	—	—
MnO	0.13	0.14	0.11	0.11	0.13	0.15
NiO	0.08	0.12	0.08	0.25	—	—
	100.62	100.25	100.32	100.40	99.16	99.30

Remarks:

(*a*) Olivine pyroxenite, 400 m SE of Army Leave Camp, Troodos: Wilson (1959), table II, Analysis 1155, p. 85.
(*b*) Olivine-rich pyroxenite, Trooditissa, Platres-Prodomos Road: Wilson (1959), table II, Analysis 1154.
(*c*) Dunite, 1.6 km west of Troodos Village: Wilson (1959), table II, Analysis 628.
(*d*) Harzburgite, 1.6 km west of Troodos Village: Wilson (1959), table II, Analysis 625.
(*e*) Harzburgite, Limassol Forest area: Pantazis (1967), table V, Analysis 8611, p. 89.
(*f*) Serpentinite, Limassol Forest area: Pantazis (1967), table V, Analysis 8608, p. 89.

Phase layering in the gabbro is common, especially in pyroxene and olivine gabbros. Some is clearly cumulate in origin; some shows features characteristic of flow layering (Thayer 1963) but may be deformed cumulate layering.

The gabbroic rocks grade downward by increasing concentration of mafic minerals into a unit of poikilitic olivine pyroxenite, pyroxenite, and felspathic olivine pyroxenite, designated by Wilson (1959) the harzburgite-wehrlite and the pyroxenite peridotite groups. Prominent layering in this unit is marked by varying proportions and grain size of pyroxene. Olivine is present as sub- to euhedral grains poikilitically included in pyroxene (see figure 16, plate 6). The abundance of olivine ranges gradationally from 20 to 70 % in different layers, and clinopyroxene is predominant only near the gabbro.

The lowermost rocks of the complex consist of dunite and harzburgite, the latter the 'enstatite olivinite' of the Cyprus Survey geologists. These rocks contain 80 to 100 % olivine with

inter-layered enstatite. Rocks are strongly foliated, the latter marked by preferred orientation olivine grains as well as centimetre scale monomineralic enstatite layers (figure 17, plate 6). These two units contrast strongly with the pyroxenite-olivine pyroxenite unit in texture and in overall outcrop appearance. Chromite is present as accessory grains and as layered concentrations within dunite bodies. Both interlayered dunite and harzburgite and chromite concentrations within dunite display isoclinal similar folds, the axes of which plunge down the dip of the layering (see figure 18, plate 6).

Table 5 shows available chemical analyses of dunite, harzburgite and olivine pyroxenite. Available mineralogic data, mostly optical (Böttcher 1969) suggests that the magnesium content in dunite and harzburgite is approximately 90 to 94 %, and 82 to 87 % in the olivine pyroxenite. In addition, it is clear from the analyses that there is a tendency toward iron enrichment in olivine pyroxenite relative to the harzburgite.

TABLE 6. COMPARISON OF CHEMICAL RANGES FROM TROODOS ROCKS, AND OTHER ALTERED VOLCANIC SEQUENCES

	Melson & Van Andel (1966) (*a*)		Smith (1968) (*b*)	Troodos (*c*)
	average fresh basalt	range of differences between greenstone and average basalt	range of values	range of values
SiO_2	49.38	−1.20 to +2.32	38.17 to 65.31	41.0 to 78.3
Al_2O_3	16.43	−0.13 to −1.73	12.18 to 18.27	4.64 to 17.6
Fe_2O_3	2.02	+0.03 to +1.89	2.13 to 9.93	1.58 to 13.5
FeO	6.98	−3.06 to +0.33	0.72 to 15.03	
MgO	8.34	−1.99 to +1.13	0.20 to 5.99	0.57 to 33.45
CaO	11.26	−4.82 to +1.30	3.54 to 22.40	0.92 to 14.32
Na_2O	2.74	+0.19 to +1.74	0.03 to 6.55	0.25 to 4.8
K_2O	0.28	−0.17 to −0.23	0.01 to 3.98	0.04 to 4.85
H_2O^+	0.63	—	—	—
H_2O^-	0.45	—	—	—
TiO_2	1.32	−0.41 to +0.42	0.42 to 1.63	0.12 to 1.34
P_2O_5	0.25	−0.07 to +0.02	0.24 to 1.50	0.11 to 0.19
MnO	0.15	—	0.06 to 0.28	0.03 to 0.35

Remarks:

(*a*) Data adapted from Melson & Van Andel (1966), table VII, p. 177.
(*b*) Data adapted from Smith (1968), table III, pp. 204–207.
(*c*) Data from tables 1–3, this paper.

COMPARISON WITH ROCKS FROM OCEANIC AREAS

The chemical variations of pillow lavas and associated intrusives are given above. Compared with basaltic and metabasaltic rocks dredged from the oceans, Troodos rocks display a similar range of SiO_2 content, alkalis and K_2O (see Melson & Van Andel 1966; Aumento 1968, 1969; Aumento & Loncarevic 1969; Aumento *et al.*, this volume, p. 623; Muir & Tilley 1966, 1964). The degree of metamorphism and possible contamination in pillow lavas and Basal Group is reminiscent of that found by Smith (1968) in burial-metamorphosed basaltic flows in Australia. Table 6 shows the range of chemical variation found by Smith together with that found by Melson & Van Andel, as well as ranges for Troodos rocks. Such a comparison is not necessarily meaningful, but it is clear from Smith's work that low-grade metamorphism and metasomatism such as suffered by Troodos rocks, is a very complex chemical phenomenon, which is of major

importance when comparing chemical data from altered volcanic piles. Consequently we feel that the chemical similarities or discrepancies between the altered Troodos and known fresh or altered oceanic rocks is neither an argument for nor against their origin at an oceanic ridge, but is an indication of a complex subsequent diagenetic and metamorphic history.

Another problem with the Troodos rocks when compared to oceanic rocks is the general lack, except for the Upper Pillow Lavas, of fresh or altered olivine phenocrysts or xenocrysts. There is no ready answer to this apparent discrepancy. Possibly some chlorite or celadonite alteration may be derived from olivine; some patches of secondary mafic minerals could be interpreted as having outlines resembling relict olivine crystals.

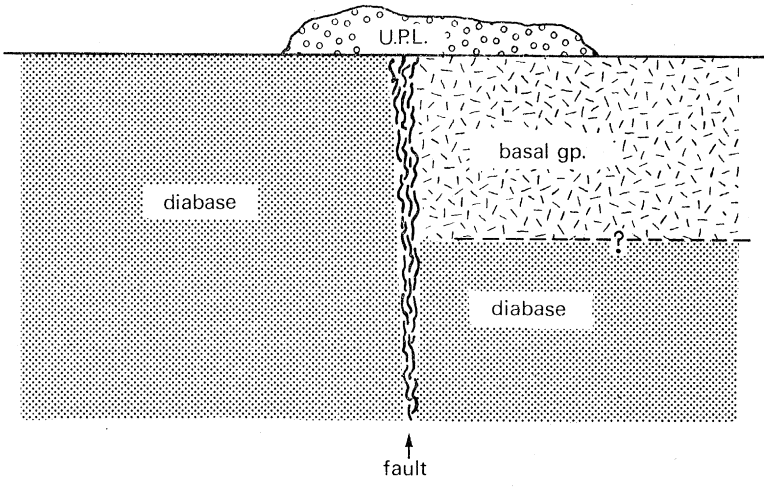

FIGURE 19. Cross-sectional sketch of relations on postulated Fossil Transform Fault. Sketch made looking eastward.

In summary, we feel that though the chemical and petrographic information available for the Troodos Complex differs somewhat from that for oceanic material, the effects of more comprehensive sampling of the various crustal units on Cyprus and of possibly differing post-magmatic chemical and mineralogic changes are not known with enough certainty to assess the significance of these discrepancies. On the other hand, the structural features of the Troodos Complex, in particular the dyke swarm, are readily compatible with origin by spreading at a ridge crest.

POSSIBLE FOSSIL TRANSFORM FAULT

The east–west trending fault zone interpreted as a fossil transform fault is shown on figure 1. The main characteristics of this feature are: (1) a broad, straight valley extending for 30 km or more; (2) a zone of brecciation as much as 100 to 200 m wide, along which Basal Group or Lower Pillow rocks are juxtaposed against Diabase; (3) a change in strike of dykes from mostly north–south to mostly east–west as one approaches the zone; (4) the presence of Upper Pillow Lavas in several places unconformably overlying faulted Lower Pillow Lavas, Basal Group and Diabase (see figure 19); (5) a zone of talus breccia with fragments of Diabase and some pillow lava, which is closely associated with the fault zone.

We interpret these features as resulting from transform movement during formation of the Basal Group, Lower Pillow Lava, and Diabase and prior to extrusion of the Upper Pillow Lavas. The presence of the east–west striking dykes in this region suggests intrusion along the fault zone.

Tectonic emplacement of the Troodos Massif

Subsequent to its formation about a postulated mid-Tethyan ridge, the Troodos Complex was caught up in the orogenic movements which gave rise to the Tehyan Mountain system. Gass & Masson-Smith (1963) and Bagnall (1964) have postulated thrusting over the African shield. The major tectonic emplacement was preCampanian in view of the widespread and generally undeformed Campanian chalks surrounding the mass. Minor subsequent late Tertiary movements have uplifted the massif and thrust it southward over the chalks. Possibly the main emplacement of the massif resulted from the collision of the African continent with a subduction zone dipping to the north (Temple & Zimmerman 1969; D. H. Roeder, personal communication). The Mamonia melange, which underlies the chalk sediments southwest of the Troodos Complex, may represent this fossil subduction zone or debris derived from it.

Magnetic properties

An indication of the direction and intensity of the natural remanent magnetization (n.r.m.) of over 900 hand specimens, from 150 localities within the Troodos Complex, has been obtained in the field with a portable fluxgate magnetometer (Doell & Cox 1967). In addition, a total of 200 oriented drill cores were obtained from 27 sites for further laboratory study. From previous experience with basic rocks it was felt that the direction of n.r.m. could be assessed in the field to within 20° of the true direction. This supposition was amply confirmed by the subsequent laboratory measurements of n.r.m. Moreover, in general, the directions of the remanent magnetic vectors for both mafic and ultramafic rock types change very little as a result of thermal or alternating field demagnetization treatment. Thus the n.r.m. directions obtained in the field can usually be taken to be indicative of the primary remanent magnetization. This feature of many of the rocks studied was clearly of great value in assessing preliminary results in the field, extending the area covered by magnetic sampling, and increasing the number of local or specific structural problems which could be investigated by the paleomagnetic method.

Obviously a primary objective of the project was to determine the distribution and extent of interfingering of normally and reversely magnetized material within the complex, in the hope of simultaneously confirming the validity of the Vine–Matthews hypothesis and providing compelling evidence that the massif was indeed formed by the process of sea-floor spreading. However, much to our chagrin no areas of convincingly or consistently 'reversed' material have been found, despite a fairly comprehensive reconnaissance survey of the main outcrop area and the two major inliers at Akamas and Troulli. If the complex represents a fragment of oceanic crust generated at a mid-ocean ridge crest, then the 110 km across strike extent of the outcrop area would represent between 11 and 5.5 Ma of spreading history if the ridge were spreading at a rate of 1 to 2 cm a^{-1} per ridge flank as suggested below. Such long epochs of consistently normal polarity of the Earth's magnetic field are thought not to occur during the late Cretaceous and Tertiary (Heirtzler *et al.* 1968) but may in the early and middle Cretaceous. Helsley & Steiner (1969) have suggested, on the basis of palaeomagnetic studies on land, that there are two such intervals, one of 20 and the other of 30 Ma duration, during this period. Although equivocal, it seems most probable, from the available evidence, that the Troodos Massif is middle Cretaceous in age. This conclusion is based on the Campanian age assigned

to the faunal assemblage in the overlying radiolarian shales (Allen 1967) and preliminary potassium–argon age determinations (I. G. Gass, personal communication).

The pillow lavas and gabbros, which show little or no subsequent alteration, are thought to preserve their primary thermo-remanent magnetization. Clearly no 'reversal test' can be applied to the paleomagnetic vectors derived from these rocks but the results obtained are of considerable interest in that they yield a dip which is what one would expect for Cyprus during the Cretaceous, from extrapolation of African or European data (see, for example, Irving 1967), but a declination that is approximately due west. Such an azimuth for the palaeomagnetic vector is completely unexpected and most simply interpreted as indicating an anticlockwise rotation of the whole massif through approximately 90° since the time of its formation. This would imply formation at a ridge crest trending east–west, since the present predominant strike direction or 'grain' is north–south, and is more readily compatible with the assumed east–west elongation of the Tethys (Gass 1968).

The remobilized serpentinites yield randomly orientated and unstable remanent vectors, but the non-remobilized harzburgite and dunite units of the Plutonic Complex yield vectors which are stable and approximate to the present direction of the Earth's magnetic field. This stable remanence is presumably a chemical remanence acquired during serpentinization (cf. Saad 1969) and its direction implies that serpentinization is perhaps related to the late Tertiary uplift and emplacement of the massif. This observation and interpretation lends added credence to the correlation of these ultrabasics with submoho material since in an unserpentinized condition their densities would correspond to those inferred from the submoho velocity of 8.1 km s^{-1} for compressional seismic waves, i.e. 3.3 to 3.4 g cm^{-3} (Hess 1962; Talwani, Le Pichon & Ewing 1965). Many of these rocks, at present, have densities of 3.0 to 3.1 g cm^{-3} implying less than 50 % serpentinization. Thus we postulate that some ultramafic rocks dredged from the ocean floor might be derived from small, isolated pockets within the crust but most represent remobilized serpentinite which has been tectonically emplaced along fractures. The highly fractured nature of crust generated at more slowly spreading ridge crests, e.g. in the Atlantic and north-west Indian Oceans, may account for the fact that serpentinites are commonly dredged in these areas, but never in the Pacific.

The intensity of n.r.m. for the pillow lavas is typically of the order of 10^{-2} e.m.u. cm^{-3} and the Koenigsberger ratio (Q_n) $\sim$ 10, i.e. the n.r.m. intensity is on average ten times greater than the intensity of induced magnetization, as is the case for ocean floor basalts (e.g. Opdyke & Hekinian 1967). In contrast, the greenschist facies rocks (Basal Group and Diabase) have similar magnetic susceptibilities, i.e. intensities of induced magnetization $\sim 10^{-3}$ e.m.u. cm^{-3}, but Koenigsberger ratios of approximately 0.5. This drastic reduction in the intensity of the remanent magnetization is to be expected since the metamorphic process involves destruction of many of the primary iron–titanium oxide phases—titanium for example being taken up in newly formed sphene. This makes recovery of the primary remanent direction from these rocks very difficult and the directions of their remanent vectors are generally intermediate between those of the pillow lavas and gabbros and the present direction of the Earth's magnetic field. Presumably secondary viscous components of remanence are now comparable in intensity and stability to those of the residual primary remanence. The plutonics have natural remanent intensities of order 10^{-3} e.m.u. cm^{-3} and Koenigsberger ratios of approximately 1, the gabbros and diorites being more consistent in this respect than the ultramafics, which are highly variable.

Thus, pursuing the sea-floor analogue, the most potent sources of remanent magnetization

contrasts within the oceanic crust are seen to reside in the upper part, the pillow lavas or seismic layer two, as suggested by Vine & Wilson (1965) and many others subsequently. Originally it was thought that layer three might be less effective in this respect because it consists of gabbro or serpentinite, but it now seems probable, both from more recent dredge hauls and the analogy with Troodos, that the upper part of layer three (Diabase) and lower part of layer two (Basal Group) consist of greenschist facies dolerites equally impotent as regards contributing to the magnetic anomalies observed at or above sea-level.

More detailed documentation and consideration of the magnetic results was considered inappropriate to this meeting and will appear elsewhere.

Discussion

Isoclinal folds, pronounced foliation, and preliminary petrofabric analysis of dunite and harzburgite suggest that these rocks are tectonites, rather than primary crystalline phases. We interpret these rocks as representing upper mantle material which has flowed in a solid state upward into an opening crack. The olivine pyroxenites, gabbros, Sheeted Complex and pillow lava rocks represent either the products of fractional fusion, segregated from parent mantle material during upward flow at a mid-ocean ridge, or fractional crystallization of such fusion products subsequent to their emplacement in the oceanic crust. Some layered gabbro-pyroxenite bodies clearly are of cumulate origin resulting from crystallization of small intrusive bodies of mafic magma. Some uralitized gabbro and quartz diorite are the residual liquids of such a process. Other masses of pyroxenite, gabbro, and quartz diorite show no such clear relation to one another, and may be partial fusion products of different compositions.

Figure 20 shows a schematic cross-section of the Troodos Complex. Several implications of this interpretation are as follows:

(1) The more olivine-rich Upper Pillow Lavas may have their source from the olivine pyroxenite zone near the Moho. Such a conclusion is supported by their more ultramafic composition (see tables 1 and 5), and by the presence in the Sheeted Complex and Lower Pillow Lavas of small possibly pipe-like intrusions of olivine pyroxenite (see maps in Bear 1960; Gass 1960; and Wilson 1959).

(2) The observed field relations are best interpreted as the product of multiple intrusion and extrusion of small portions of liquid. Such a concept is supported by the abundant presence of chilled margins and multiply-intruded dyke complexes, the mutually contradictory relations between gabbro and diabase, with each intruding, and intruded by the other, and the presence of some apparently rootless dykes in the gabbro and diabase (L. M. Bear, oral communication, 1969). Such multiple intrusion and multiple chilling effects imply the emplacement of material, hence extension over a fairly broad zone, and a slow enough rate of spreading to allow for the production of chilling effects. This suggests that the ridge must have been fairly slow-spreading.

(3) The relief of the zone of maximum dyke formation—the top of the Sheeted Complex—and the presence of both vertical and conjugate dyke systems possibly are related to varying rates of magma supply and extension. Vertical dykes possibly suggest a role for fluid pressure and forceful injection of dyke material, causing the rock to fracture perpendicular to minimum compressive stress. On the other hand, if the rock is first extended by normal faulting and subsequently intruded, then conjugate systems of dykes may be formed. In addition, if the rate

PHILOSOPHICAL TRANSACTIONS OF THE ROYAL SOCIETY A MATHEMATICAL, PHYSICAL & ENGINEERING SCIENCES

of supply of magmatic material to the ridge axis is relatively large in relation to extension, then one might expect a relatively greater thickness of flows above and sill-like intrusions of gabbro below, a relatively thick Lower Pillow Lava and Basal Group (or Layer Two), and a relatively thin Sheeted Complex. If, on the other hand, the rate of creation of volume by extension gets slightly ahead of rate of supply of magmatic material to the ridge, one would expect a slightly thinner layer two crust, and a relatively greater proportion of sheeted material, perhaps as suggested for the East Pacific Rise by Menard (1967).

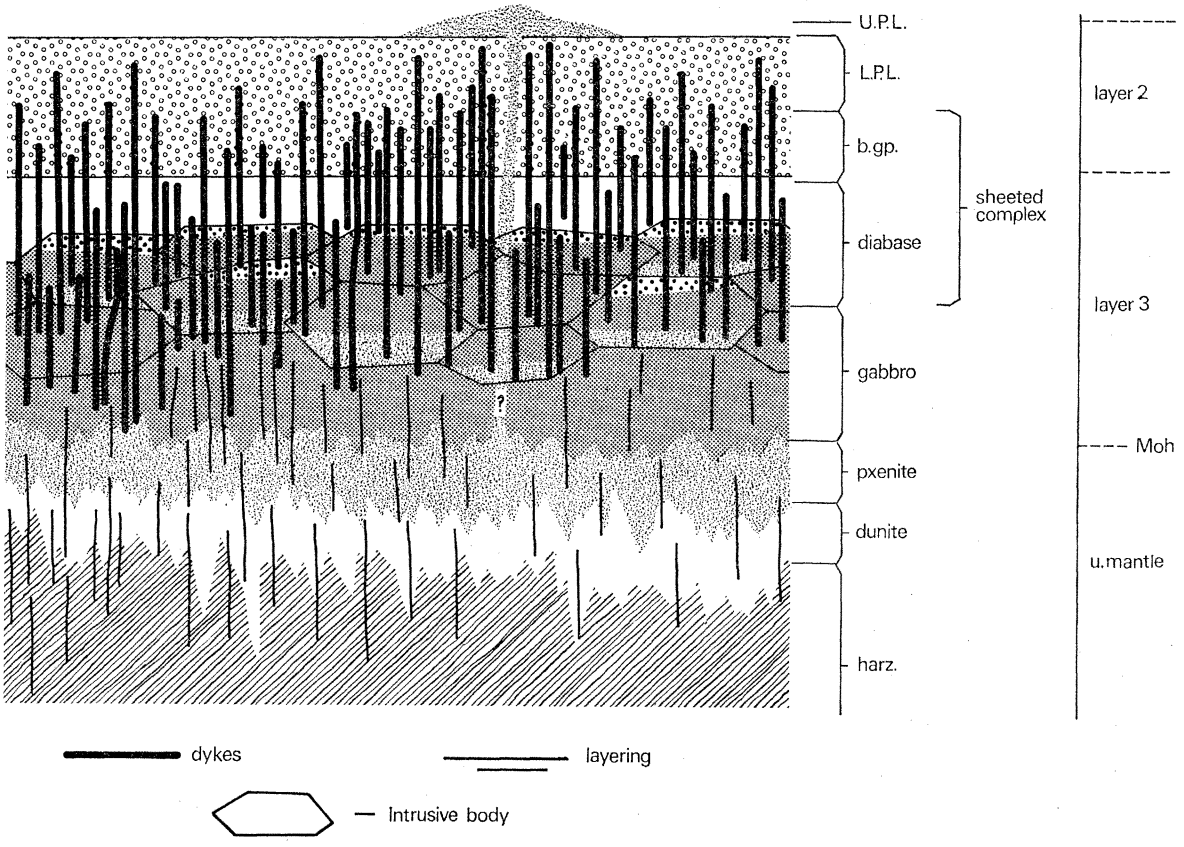

FIGURE 20. Interpretative cross-section of Troodos Complex. Large closed dots are quartz diorite-granophyre segregations in gabbro bodies. Open dots are pillow lava. Heavy black lines are dykes. Column to right is postulated correlation with seismic layers of the oceanic crust.

OTHER SHEETED COMPLEXES

It is now apparent that the Troodos Complex is not unique in exhibiting a sheeted diabase complex. Other complexes which have this or similar features are as follows:

(1) *Kizil Dagh, Hatay, Turkey.* Dubertret (1955) described a reconnaisance survey of this mass, and particularly referred to 'stratified beds' of dolerite, now dipping vertically. Recent reconnaisance of this exposure by Vuagnat & Çogolu (1968) and ourselves confirmed the presence of a sheeted complex.

(2) *Oman Mountains.* Reinhardt (1969) has summarized features of the Oman Mountains geosyncline in which he shows (his p. 5 and 27) subvertical Diabase dyke swarms, again suggesting similarities to Troodos.

(3) *Macquarie Island.* Varne *et al.* (1969) have described in the northern part of the island the presence of strip-like exposures of harzburgite, layered gabbro and sheeted Diabase intruded into a basaltic sequence.

In contrast to the above examples, however, most Diabases from ophiolite complexes have not been described as exhibiting sheeted structure, but as consisting of two main types: first, exemplified by the Vourinos Complex, northern Greece (see figures 21 and 22), where internal layering is parallel, rather than perpendicular, to major rock units; secondly, such as in the Italian occurrences, where no particular internal structure has been described (see figure 23). The Vourinos Complex (Moores 1969) displays a substantial development of phase and cryptic-layered pyroxenite, gabbro, and diorite, suggesting some intrusion and cumulate formation.

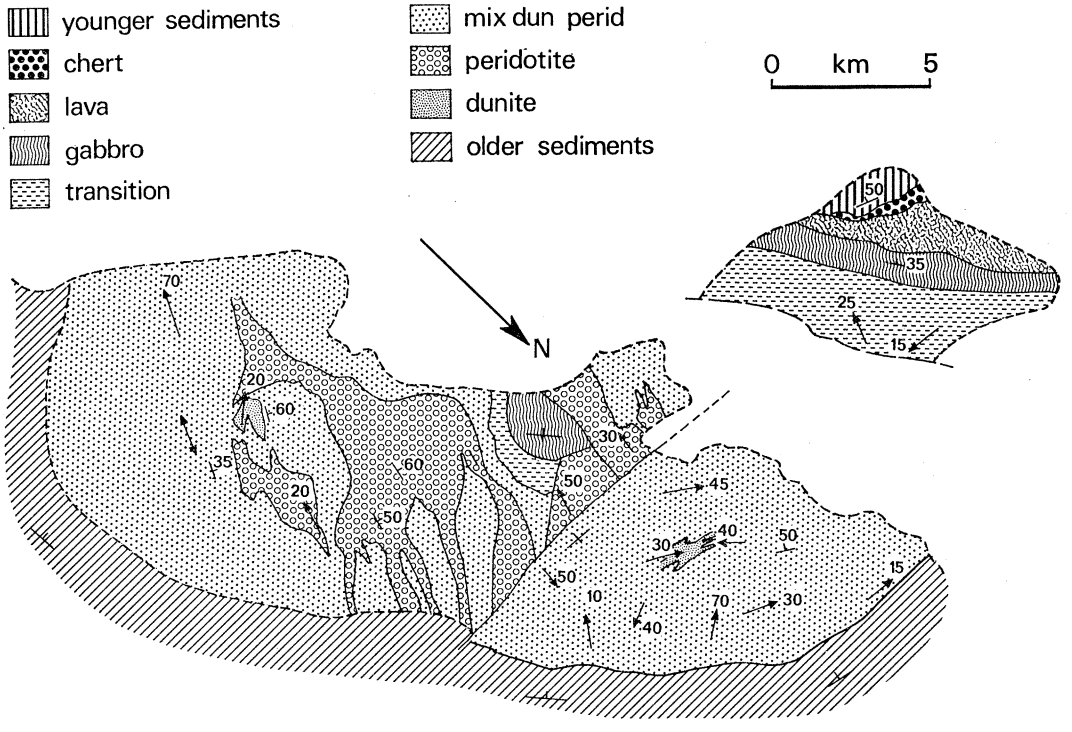

FIGURE 21. Map of Vourinos Complex, northern Greece, after Moores (1969). Attitudes are of foliation and minor fold axes.

Many Italian bodies (J. C. Maxwell 1969, 1970, and oral communication) contain peridotite or serpentinized peridotite, thin or absent gabbro, diabase without internal layering or dyke structure which grades non-descriptly into pillow lava or extrusive breccia. Though presently unexplained, these differences in internal structure apparently are primary and fundamental features. If these other ophiolites represent fragments of oceanic crust, then these differences in internal structure may represent differences in behaviour on spreading ridges. In speculating on a possible analogy with modern oceanic ridges, the difference in topography between slow and fast-spreading ridges (Menard 1964, 1967; Van Andel & Bowin, 1968) comes to mind. The generally prominent median valley and rugged topography of slow-spreading ridges such as the Mid-Atlantic and the northwest Indian Ocean Ridges contrast strongly with the smooth topography of the fast-spreading East Pacific Rise. The possible slow-spreading ridge origin of the Troodos Complex has been outlined above. Perhaps ophiolites without marked internal

PHILOSOPHICAL TRANSACTIONS OF THE ROYAL SOCIETY A MATHEMATICAL, PHYSICAL & ENGINEERING SCIENCES

structure represent crust and mantle formed as fast-spreading ridges, such as the East Pacific Rise, where all material would be injected in a narrower axial region (Vine 1968), and when injected, would move out without further addition, crystallizing as it moved. In this case, the upper part of the injected magma would crystallize immediately and display extrusive features, and the part immediately underlying it would crystallize more slowly and show gradation downward into coarser-grained intrusive material.

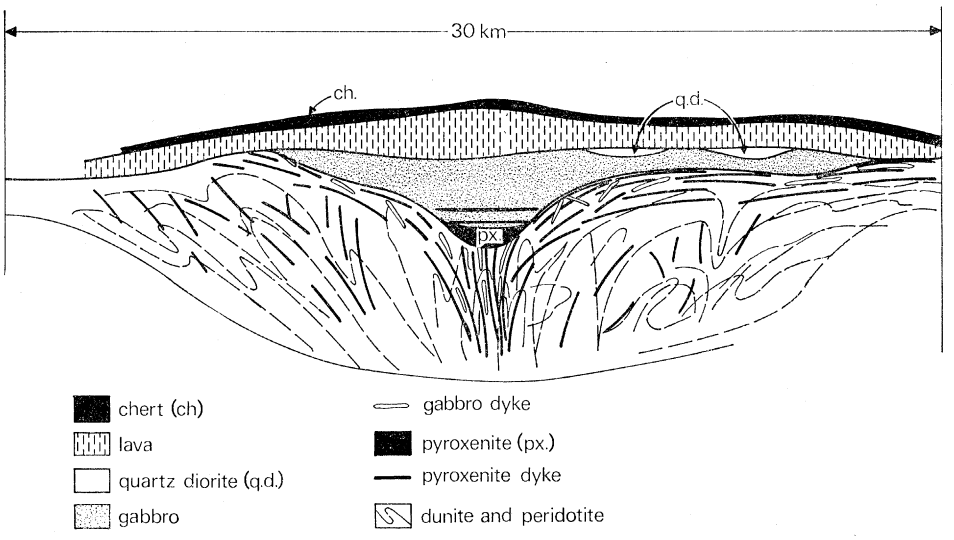

FIGURE 22. Schematic cross-section of Vourinos Complex, after Moores (1969) showing complex structure of ultramafic rocks plunging towards the centre, pyroxenite and gabbro dykes concentrated towards the centre, and overlying mafic rocks.

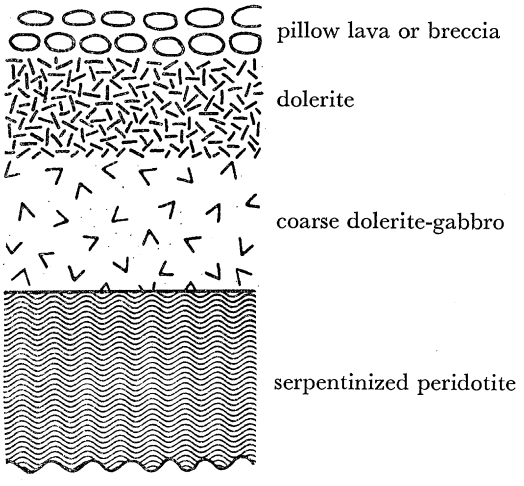

FIGURE 23. Schematic cross-section of Italian ophiolite complex, after J. C. Maxwell (personal communication).

The fact that successive intrusions in the Sheeted Complex and Lower Pillow Lava commonly dissect pre-existing dykes has been outlined above. This is an important relation, for it suggests that the intrusion process is not entirely random, at least on a short time scale, e.g. a few thousand years (4 m dykes intruded and repeatedly dissected every 200 years is equivalent to a half-spreading rate of 1 cm a^{-1}). Hence the process of emplacement invoked for fast-spreading

ridges was operative at least locally on Troodos, and yet chilled contacts are developed on Troodos. The obvious difference, however, is the rate of emplacement of material. If the discrete volumes injected are the same in both cases, intrusives on fast-spreading ridges (e.g. East Pacific Rise) would be several times more frequent. Perhaps two effects are operative: (1) a narrower zone of injection over a long time span on a fast-spreading ridge, which would tend to make the central zone of formation hotter and narrower; and (2) a higher frequency of intrusion in fast-spreading ridges, which would tend to maintain higher temperatures at the ridge crest and prevent the formation of chilled contacts. Possibly the Vourinos Complex, which displays some differentiation and also parallel internal structure, represents a stage intermediate between the 'fast-spreading' Italian ophiolite and 'slow-spreading' Troodos models. The internal fabric of the ultramafic rocks also differs. On Troodos foliations of dunite and harzburgite are vertical, whereas in Vourinos they were originally horizontal away from the divergent and complexly domed centre. This difference implies that mantle layering on slow-spreading ridges tends to be vertical and becomes horizontal on fast-spreading ridges. Under this interpretation, the divergent structure present in the Vourinos Complex implies that it represents a piece of *the actual crest* of the former mid-Tethyan ridge. The zone of vertical dykes in the centre of the complex then would represent the zone of dyke intrusion at a ridge and the complexly domed ultramafics in the same area may represent fossil mantle diapirs.

The model outlined above is clearly speculative, but seems to be compatible with the known petrology and structure of Tethyan ophiolites. It provides a means of reconciling the three conflicting hypotheses for the origin of ophiolites outlined in the Introduction. If the model is correct, then it means that dyke intrusion, stratiform crystallization in magma chambers, and solid diapiric activity all occur at a ridge crest. Subsequently fragments of crust and uppermost mantle formed in this manner are thrust upon a continental margin. The conflicting interpretations of origin of ophiolites have resulted from study of individual occurrences in which these features have been variously preserved.

Throughout this study we drew on the experience and benefited from the advice and assistance of Dr L. M. Bear, formerly member and director of the Cyprus Geological Survey (1955–64) and of the U.N. Mission in Cyprus (1965–9). Especially valuable was his excellent grasp of the details of geology of the Troodos Massif, acquired over 14 years of enthusiastic observation.

We would also like to thank Dr Y. Haji Stavrinou, Director of the Cyprus Geological Survey, and many members of his staff, particularly Dr Theo Pantazis, for their hospitality, assistance and interest. We benefited from discussions with H. L. Davies, A. Gansser, I. G. Gass, H. H. Hess and J. C. Maxwell.

This study was supported by National Science Foundation Grants GA-1257 and GA-1395

References (Moores & Vine)

Allen, C. G. 1967 *Ann. Rep. Geol. Surv. Dep. Cyprus for* 1966, p. 8.
Aubouin, J. 1965 *Geosynclines*. New York: Elsevier.
Aumento, F. 1968 *Can. J. Earth Sci.* **5**, 1–22.
Aumento, F. 1969 *Science, N.Y.* **165**, 1112–1113.
Aumento, F. & Loncarevic, B. D. 1969 *Can. J. Earth Sci.* **6**, 11–23.
Bagnall, P. S. 1960 *Geol. Surv. Cyprus Mem.* **5**, 1–116.
Bagnall, P. S. 1964 *J. Geol.* **72**, 327–345.
Bear, L. M. 1960 *Geol. Surv. Cyprus Mem.* **3**, 1–122.
Bear, L. M. 1965 *Geologic Map of Cyprus*, 1/250000. Cyprus: Geol. Surv. Dep.

PHILOSOPHICAL TRANSACTIONS OF THE ROYAL SOCIETY A MATHEMATICAL, PHYSICAL & ENGINEERING SCIENCES

Bear, L. M. 1966 *Ann. Rep. Geol. Surv. Dep. Cyprus for* 1965, pp. 26–37.
Bear, L. M. & Morel, S. W. 1960 *Geol. Surv. Cyprus Mem.* **7**, 1–88.
Bezone, S. P. 1969 *Geol. Soc. America, Abstracts with Programs for* 1969, **3**, 5–6.
Böttcher, W. 1969 *Neues Jb. Miner. Abh.* **110**, no. 2, 159–187.
Brunn, J. H. 1956 *Ann. Geol. Pays Hell.* **7**, 1–358.
Brunn, J. H. 1960 *Revue Géogr. phys. Géol. dyn.* **3**, 115–132.
Burri, C. & Niggli, P. 1945 *Vulkaninstitut Immanuel Friedländer Publikationen*, pp. 3–4.
Carr, J. M. & Bear, L. M. 1960 *Geol. Surv. Cyprus Mem.* **2**, 1–79.
Davies, H. L. 1969 *Int. Geol. Congr. 23rd Czech. Rep. Sect.* 1, *Proc.*, pp. 209–220.
DeRoever, W. P. 1957 *Geol. Rdsch.* **46**, 137–146.
Doell, R. R. & Cox, A. 1967 In *Developments in solid earth geophys.* **3**, pp. 159–162. New York: Elsevier.
Dubertret, L. 1955 *Notes at Memoires sur le Moyen Orient-Museé Natl. Hist. Paris* **6**, 5–224.
Engel, A. E. J., Engel, C. G. & Havens, R. G. 1965 *Bull. Geol. Soc. Am.* **76**, 719–734.
Engel, C. G. & Fisher, R. L. 1969 *Science, N.Y.* **166**, 1136.
Gansser, A. 1959 *Ec. Geol. Helv.* **52**, 659–680.
Gass, I. G. 1958 *Geol. Mag.* **95**, 241.
Gass, I. G. 1960 *Geol. Surv. Cyprus Mem.* **4**, 1–116.
Gass, I. G. 1967 In *Ultramafic and related rocks* (ed. P. J. Wyllie), pp. 121–134. New York: Wiley.
Gass, I. G. 1968 *Nature, Lond.* **220**, 39–42.
Gass, I. G. & Masson-Smith, D. 1963 *Phil. Trans. Roy. Soc. Lond.* A **255**, 417–467.
Heirtzler, J. R., Dickson, G. O., Herron, E. M., Pitman, W. C. & Le Pichon, X. 1968 *J. geophys. Res.* **73**, 2119–2136.
Helsley, C. E. & Steiner, M. B. 1969 *Earth Planet. Sci. Lett.* **5**, 325–332.
Hess, H. H. 1962 In *Petrologic studies: a volume to honor A. F. Buddington*, pp. 599–620. Geol. Soc. Am.
Hess, H. H. 1965 In *Submarine geology and geophysics, Colston Papers* **17** (ed. W. F. Whittard & R. Bradshaw), pp. 317–333. London: Butterworth.
Hsu, K. J. 1969 *Calif. Div. Mines Geol., Spec. Publ.* **35**.
Irving, E. 1967 In *Systematics Ass. Publ.* **7**, 59–76.
MacDonald, G. A. & Katsura, T. 1964 *J. Petrology* **5**, 82–133.
Maxwell, J. C. 1969 *Tectonophysics* **7**, 489–494.
Maxwell, J. C. 1970 In *The megatectonics of continents and oceans* (ed. H. Johnson). Rutgers University Press.
Maxwell, J. C. & Azzaroli, A. 1963 *Geol. Soc. Am. Spec. Paper* **73**, 203–204.
Melson, W. G. & Van Andel, Tj. H. 1966 *Marine Geol.* **4**, 165–186.
Menard, H. W. 1964 *Marine geology of the Pacific*, 271 pp. New York: McGraw-Hill.
Menard, H. W. 1967 *Science, N.Y.* **157**, 923–924.
Miyashiro, A. 1966 *Jap. J. Geol. Geogr. Trans.* **37**, 45–61.
Moores, E. M. 1969 *Geol. Soc. Am. Spec. Paper* **118**.
Muir, D. D. & Tilley, C. E. 1964 *J. Petrology* **5**, 409–434.
Muir, D. D. & Tilley, C. E. 1966 *J. Petrology* **7**, 193–201.
Opdyke, N. D. & Hekinian, R. 1967 *J. geophys. Res.* **72**, 2257–2260.
Pantazis, T. 1967 *Geol. Surv. Cyprus Mem.* **8**, 1–190.
Poldervaart, A. 1955 *Geol. Soc. Am. Spec. Paper* **62**, 119–144.
Reinhardt, B. M. 1969 *Schweiz. miner. petrogr. Mitt.* **49**, 1–30.
Saad, A. H. 1969 *J. geophys. Res.* **74**, 6507–6578.
Smith, C. H. 1958 *Geol. Surv. Can. Mem.* **290**, 132 pp.
Smith, R. E. 1968 *J. Petrology* **9**, 191–219.
Steinmann, G. 1906 *Freib. naturf. Gesell. Bericht* **16**, 18–66.
Steinmann, G. 1926 *14th Int. geol. Congr., Madrid, C.R.* **2**, 638–667.
Talwani, M., Le Pichon, X. & Ewing, M. 1965 *J. geophys. Res.* **70**, 341–352.
Temple, P. & Zimmerman, J. Jr. 1969 *Geol. Soc. Am., Abstracts with Programs for* 1969, **7**, 211–212.
Thayer, T. P. 1963 *Min. Soc. Am. Spec. Paper* **1**, 55–61.
Trümpy, R. 1960 *Bull. Geol. Soc. Am.* **71**, 843–908.
Van Andel, Tj. H. & Bowin, C. O. 1968 *J. geophys. Res.* **73**, 1279–99.
Varne, R., Gee, R. D. & Quilty, P. G. J. 1969 *Science, N.Y.* **166**, 230–232.
Vine, F. J. 1968 In *History of the Earth's crust* (ed. R. A. Phinney), pp. 73–89. Princeton: University Press.
Vine, F. J. & Hess, H. H. 1970 In *The sea* vol. 4 (ed. A. E. Maxwell, E. C. Bullard, E. Goldberg & J. L. Worzel). New York, London: Wiley–Interscience.
Vine, F. J. & Matthews, D. H. 1963 *Nature, Lond.* **199**, 947–49.
Vine, F. J. & Wilson, J. T. 1965 *Science, N.Y.* **150**, 485–489.
Vuagnat, H. 1963 *Geol. Rdsch.* **53**, 336–358.
Vuagnat, H. & Çogolu, E. 1968 *Soc. Phys. Hist. Natur. Geneve, C.R.* **2**, 210–216.
Wilson, R. A. M. 1959 *Geol. Surv. Cyprus Mem.* **1**, 1–135.

PHILOSOPHICAL TRANSACTIONS OF THE ROYAL SOCIETY A MATHEMATICAL, PHYSICAL & ENGINEERING SCIENCES

Phil. Trans. Roy. Soc. Lond. A. **268**, 467 (1971)
Printed in Great Britain

II. FRESH BASALTS

Dispersed element chemistry of oceanic ridge basalts

By P. W. Gast
Lamont–Doherty Geological Observatory, Pallisades, New York, U.S.A.

Rare-earth elements, Sr, Ba, K, Rb, Cs, and nickel contents for more than thirty samples of oceanic ridge basalts from 30° N in the Atlantic, Gorda Rise, and equatorial Pacific have been determined. All rare-earth abundance patterns are chondritic with some depletion in lanthanum and cerium. The abundance of the heavy rare earths varies by more than a factor of two. The variation appears to be correlated with a depletion of europium relative to other rare earths and with high iron contents and low nickel contents. Barium contents consistently reflect the variations in lanthanum and cerium.

The variations in trace element content within the oceanic ridge basalt group can be quite readily explained by the crystallization of plagioclase and olivine in the approximate proportions of 4:1.

The overall chemistry of the parental oceanic ridge liquid is explained in terms of extensive partial melting at depths of 15 to 25 km. It is shown that this is the expected behaviour of mantle material with low water contents ($\sim 2\%$) undergoing an adiabatic decompression. The localization of rocks with the unusual compositions found on the oceanic ridge is ascribed to the localization of large-scale vertical movement in the mantle to these regions.

PHILOSOPHICAL TRANSACTIONS OF THE ROYAL SOCIETY A MATHEMATICAL, PHYSICAL & ENGINEERING SCIENCES

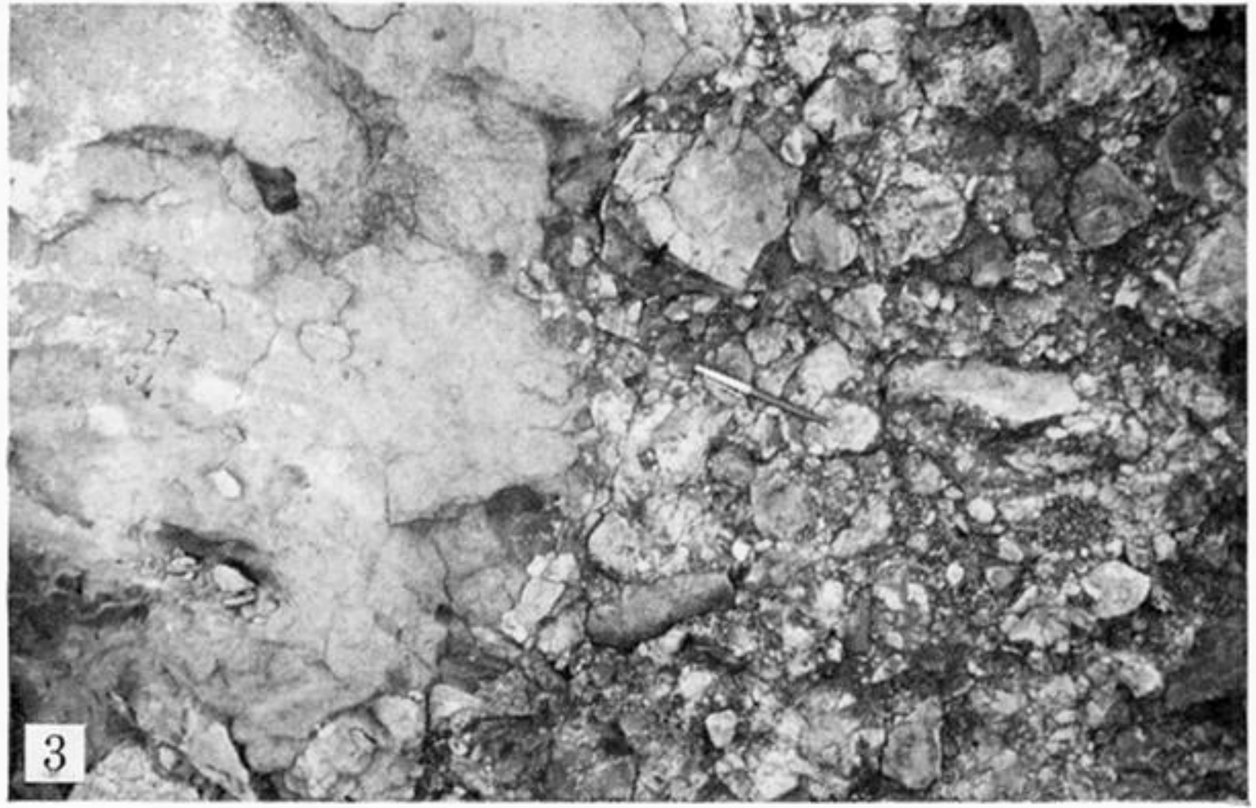

FIGURE 2. Exposure of Upper Pillow Lavas. Note intrusive-free exposure, hyaloclastic matrices between pillows, veining of calcite and analcite. Northwest margin of the massif.

FIGURE 3. Photo of breccia in Upper Pillow Lava, near southeastern margin of massif.

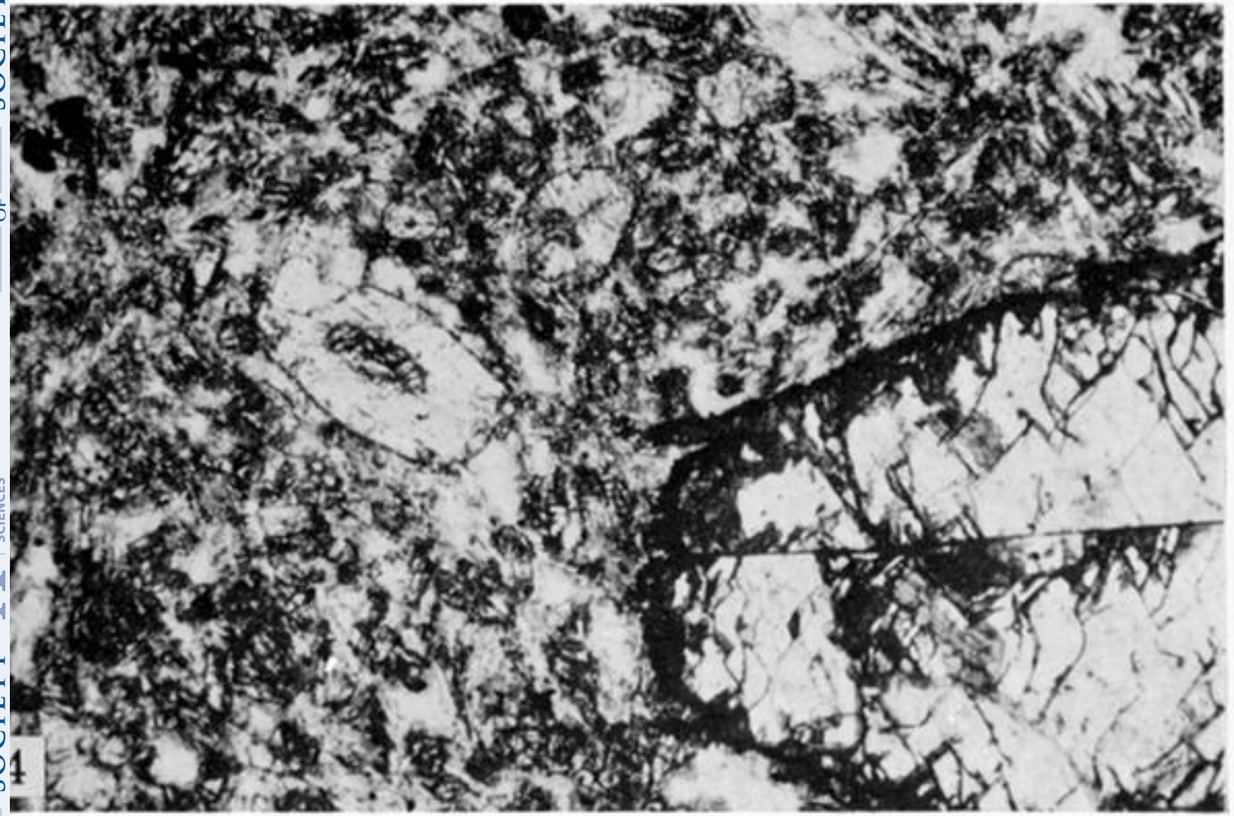

FIGURE 4. Photomicrograph of Upper Pillow Lava rock. Phenocrysts are calcite replacements of olivine in microcrystalline to glassy altered groundmass. Plain light, max. dimension 1.6 mm.

FIGURE 6. Photomicrograph of dyke intrusive into Lower Pillow Lavas. Plagioclase and augite microphenocrysts in a seriate groundmass of plagioclase and alteration products. Crossed Nicols, max. dimension 3.2 mm.

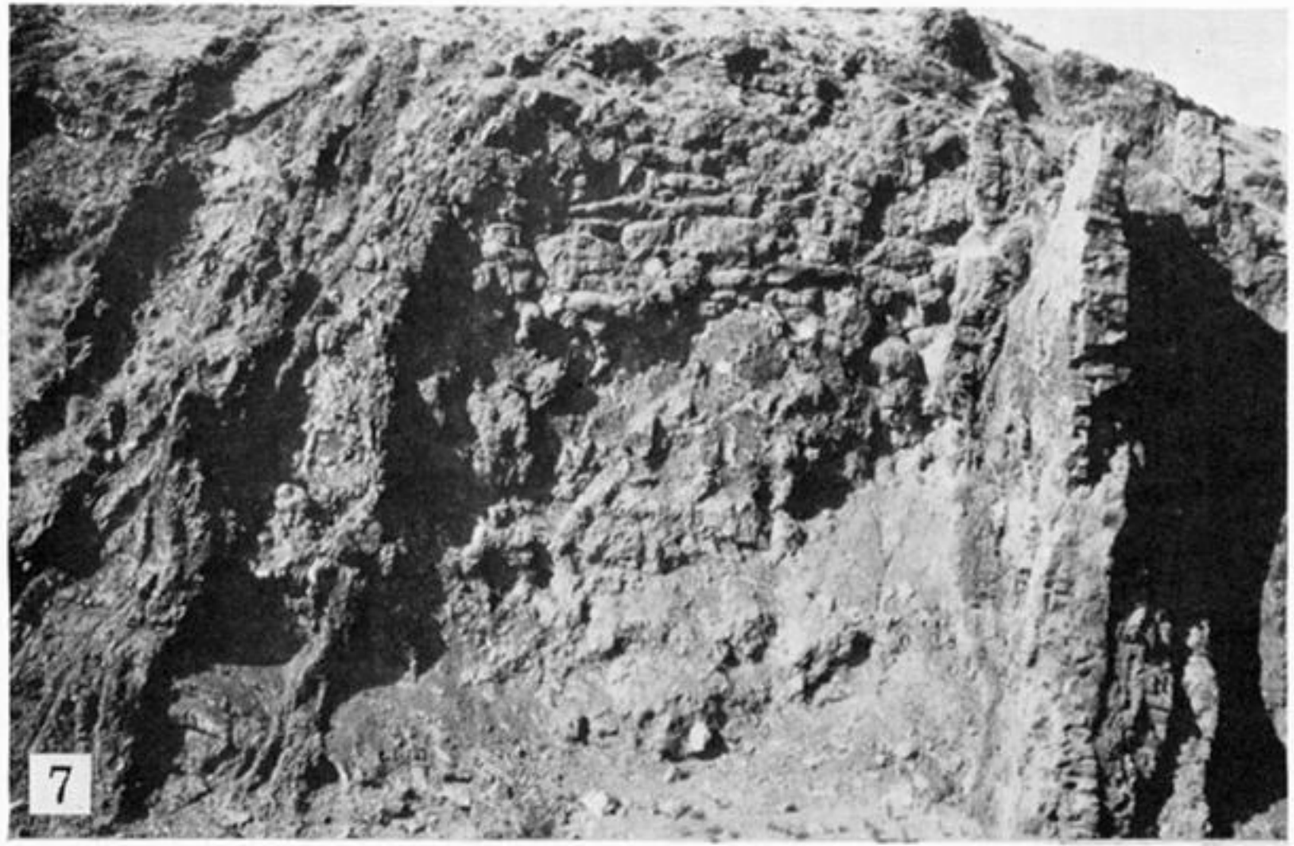

IGURE 7. Stream exposure of Lower Pillow Lavas, near contact with Sheeted Complex. Note composite dykes intruding flat-lying pillow lavas. Area below distinctive pillow structure is brecciated pillow lavas intruded by numerous small irregular sills.

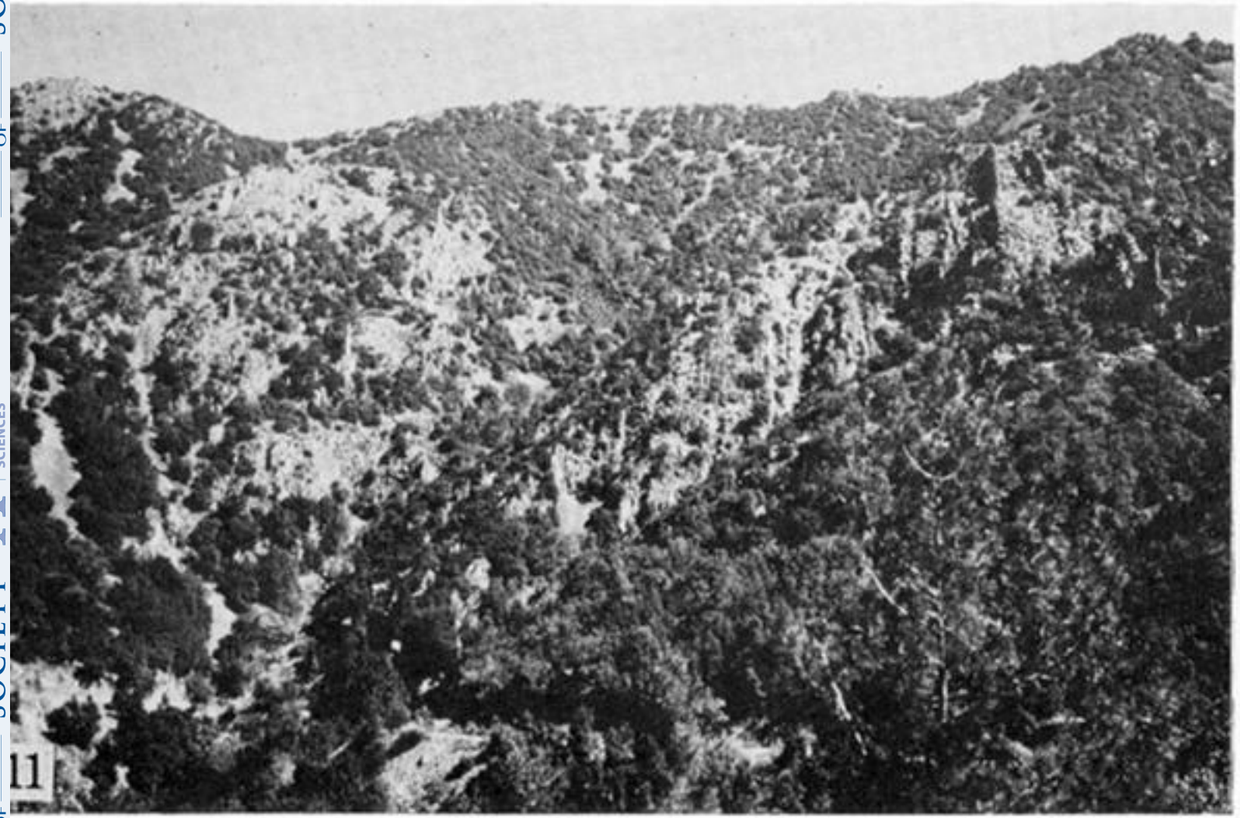

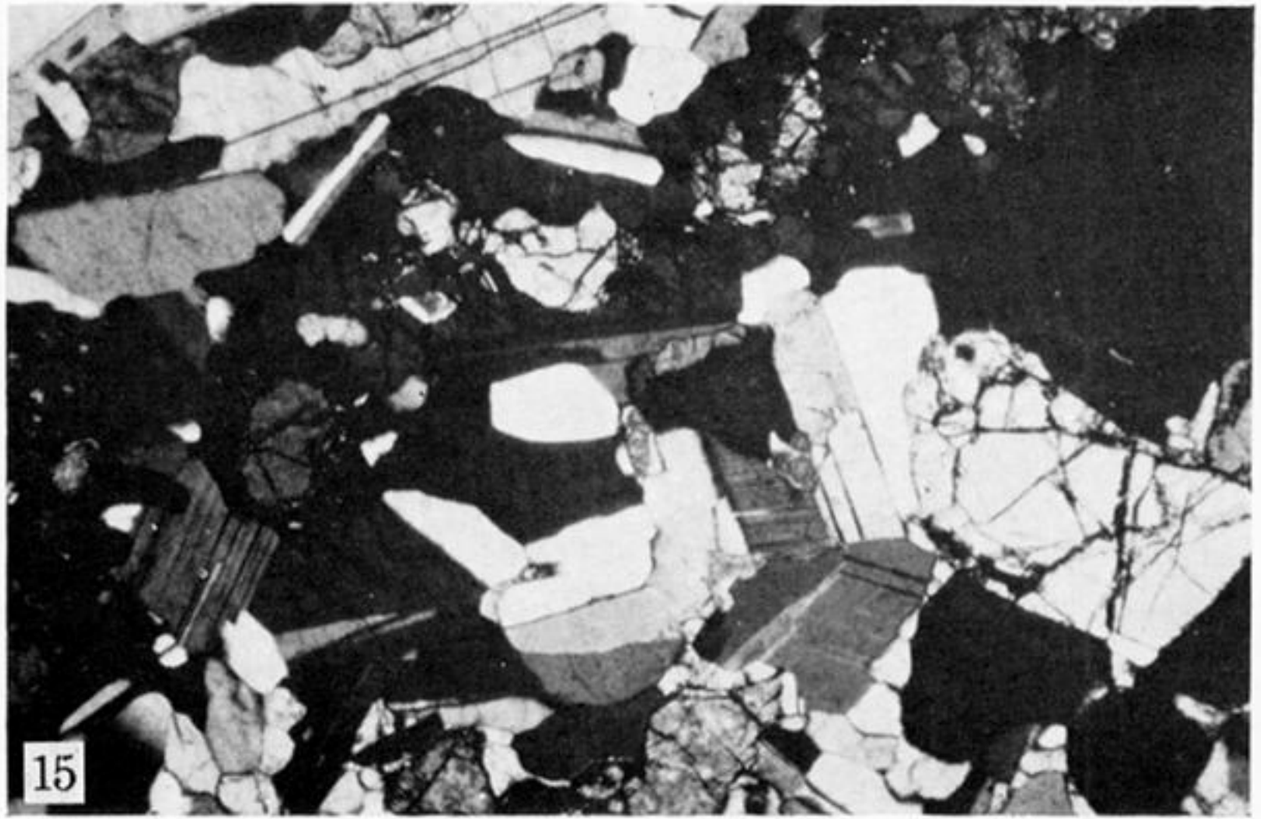

FIGURE 11. Photo of Sheeted Diabase showing typical aspect. Max. width of photo approx. 1.5 km.

FIGURE 15. Photomicrograph of olivine gabbro, labradorite, olivine, augite, and iron ore. Crossed Nicols, max. dimension 3.2 mm.

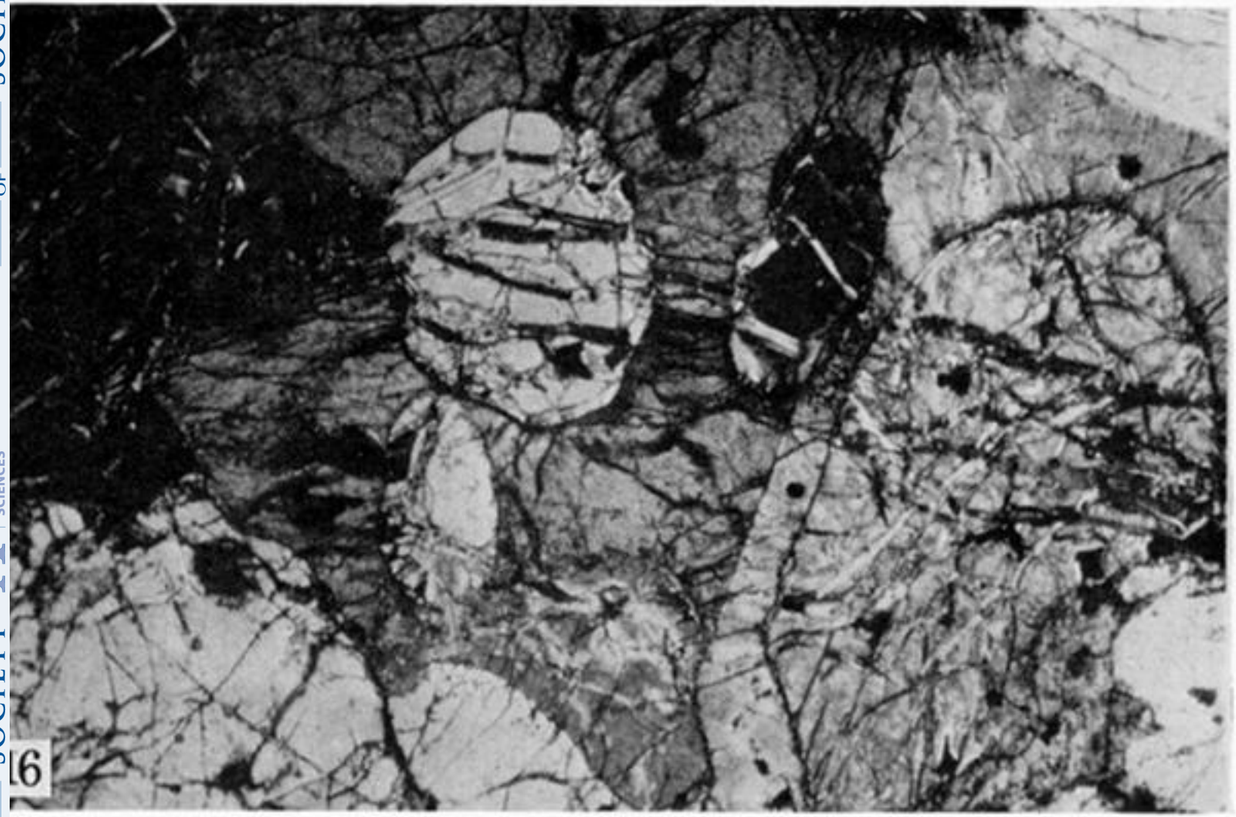

FIGURE 16. Thin section of cumulate-textured olivine pyroxenite. Subhedral olivine, anhedral, twinned, poikilitic augite. Crossed Nicols, max. dimension 3.2 mm.

FIGURE 17. Foliated harzburgite. Fabric marked by planar orientation of olivine grains and enstatite layers. Troodos ultramafic area.

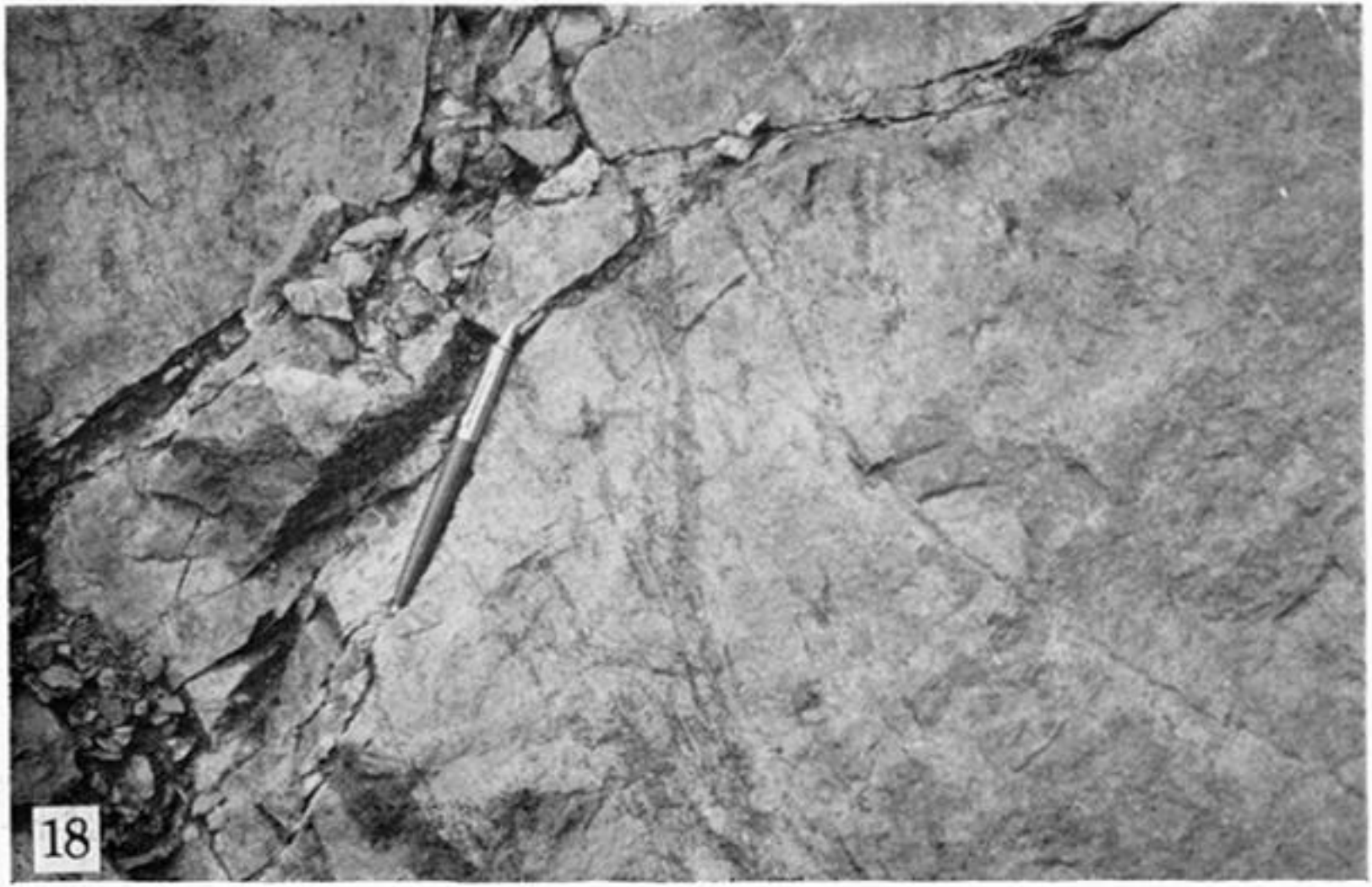

FIGURE 18. Isoclinal fold in dunite and chromitite. Troodos ultramafic area.